ABSTRACT

Title of Document: QUANTIFICATION OF ERROR IN AVHRR
NDVI DATA

Jyoteshwar R. Nagol, Ph.D., 2011

Directed By: Dr. Stephen Prince
Department of Geography

Several influential Earth system science studies in the last three decades were based on Normalized Difference Vegetation Index (NDVI) data from Advanced Very High Resolution Radiometer (AVHRR) series of instruments. Although AVHRR NDVI data are known to have significant uncertainties resulting from incomplete atmospheric correction, orbital drift, sensor degradation, etc., none of these studies account for them. This is primarily because of unavailability of comprehensive and location-specific quantitative uncertainty estimates.

The first part of this dissertation investigated the extent of uncertainty due to inadequate atmospheric correction in the widely used AVHRR NDVI datasets. This was accomplished by comparison with atmospherically corrected AVHRR data at AErosol RObotic NETwork (AERONET) sunphotometer sites in 1999. Of the datasets included in this study, Long Term Data Record (LTDR) was found to have least errors (precision=0.02 to 0.037 for clear and average atmospheric conditions)

followed by Pathfinder AVHRR Land (PAL) (precision=0.0606 to 0.0418), and Top of Atmosphere (TOA) (precision=0.0613 to 0.0684).

`   Although the use of field data is the most direct type of validation and is used extensively by the remote sensing community, it results in a single uncertainty estimate and does not account for spatial heterogeneity and the impact of spatial and temporal aggregation. These shortcomings were addressed by using Moderate Resolution Imaging Spectrometer (MODIS) data to estimate uncertainty in AVHRR NDVI data. However, before AVHRR data could be compared with MODIS data, the nonstationarity introduced by inter-annual variations in AVHRR NDVI data due to orbital drift had to be removed. This was accomplished by using a Bidirectional Reflectance Distribution Function (BRDF) correction technique originally developed for MODIS data.

        The results from the evaluation of AVHRR data using MODIS showed that in many regions minimal spatial aggregation will improve the precision of AVHRR NDVI data significantly. However temporal aggregation improved the precision of the data to a limited extent only.

        The research presented in this dissertation indicated that the NDVI change of ~0.03 to ~0.08 NDVI units in 10 to 20 years, frequently reported in recent literature, can be significant in some cases. However, unless spatially explicit uncertainty metrics are quantified for the specific spatiotemporal aggregation schemes used by these studies, the significance of observed differences between sites and temporal trends in NDVI will remain unknown.

QUANTIFICATION OF ERROR IN AVHRR NDVI DATA

By

Jyoteshwar R. Nagol

Dissertation submitted to the Faculty of the Graduate School of the
University of Maryland, College Park, in partial fulfillment
of the requirements for the degree of

Doctor of Philosophy
2011

Advisory Committee:
Dr. Stephen D. Prince, Chair
Dr. Eric Vermote,
Dr. Shunlin Liang
Dr. Rachel T. Pinker

Preface

Parts of the material presented in this dissertation have already been published in peer-reviewed journals. The results from chapter 2 have been published in Remote Sensing of Environment, while material presented in chapter 3 is being revised for publication in the Canadian Journal of Remote Sensing. The manuscript presenting results from chapter 4 is under preparation for publication in Remote Sensing of Environment.

All the three papers have Dr. Vermote and Dr. Prince as second and third author respectively. I was responsible for all of the analysis presented in these papers as well as the manuscript development. Dr. Vermote and Dr. Prince provided detailed guidance in development of the research and in the writing process.

Acknowledgements

Table of Contents

List of Tables

List of Figures

Chapter 1: Introduction

1.1. Overview

The Advanced Very High Resolution Radiometer (AVHRR) is a meteorological sensor system onboard the National Oceanic and Atmospheric Administration (NOAA) series of polar-orbiting satellites (Kidwell 1998). The AVHRR sensor collects data in the visible, near infrared and thermal infrared wave lengths. After its capability for measuring Earth surface properties was demonstrated (Townshend and Tucker 1981; Tucker et al. 1984), these data have been used extensively for Earth system science research. The most useful features of the AVHRR dataset are: its temporal extent of nearly three decades; appropriate resolution for global and regional scale monitoring (finest resolution of local area coverage $1km^2$, and global area coverage $4.4km^2$); and the extension of the record by next generation sensors, like Visible Infrared Imager/radiometer Suite (VIIRS) (Tucker et al. 2005; van Leeuwen et al. 1999).

Many Earth surface vegetation studies make use of the visible and near-infrared channels of the AVHRR in the form of vegetation indices, chiefly the Normalized Difference Vegetation Index (NDVI). Many other AVHRR derived data products also use NDVI as a primary input, e.g., global land cover maps (DeFries et al. 1995; DeFries et al. 1999), Net Primary Production (NPP) (Prince and Goward 1995), burned area product (Barbosa et al. 1999), Fraction of Absorbed Photosynthetically Active Radiation (fPAR) (Myneni et al. 1997b), Leaf Area Index

(LAI) (Myneni et al. 1997b), land surface temperature (Jin 2004), and air temperature (Prihodko and Goward 1997).

Several influential Earth system science studies in the last three decades were based on NDVI data from AVHRR series of instruments. For example Myneni et al., (1997) and Tucker et al., (2001) used AVHRR NDVI data to show an increase in plant growth and lengthening of the growing season in northern high latitudes. Tucker et al., (1991) used these data to estimate the spatial extent of the Sahara Desert and its inter-annual variation. Slayback et al., (2003) found consistent greening in global latitudinal bands from 35° to 75° N for years 1982-1999. There are many more such examples of AVHRR NDVI based studies, which are considered significant contributions and are cited widely by the scientific community (Anyamba and Eastman 1996; Bounoua et al. 2000; Cao et al. 2004; Fang et al. 2003; Hicke et al. 2002; Ichii et al. 2002; Jia et al. 2003; Lambin and Ehrlich 1997; Lee et al. 2002; Liu et al. 1994; Lucht et al. 2002; Myneni et al. 1997a; Paruelo et al. 2004; Piao et al. 2004; Piao et al. 2003; Runnstrom 2000; Slayback et al. 2003; Stockli and Vidale 2004; Tucker et al. 2001; Vicente-Serrano and Heredia-Laclaustra 2004; Yu et al. 2003; Zhou et al. 2003; Zhou et al. 2001).

Although, AVHRR NDVI data are known to have significant uncertainties resulting from shortcomings like incomplete atmospheric correction, orbital drift, sensor degradation (El Saleous et al. 2000), none of these studies account for them. This is primarily because of unavailability of comprehensive and location specific quantitative uncertainty estimates.

Most previous investigations of uncertainty in AVHRR NDVI data (Cihlar et al. 1998; Eklundh 1995; Fensholt et al. 2006a; Fensholt et al. 2006b; Gallo et al. 2005; Goward et al. 1993; Nagol et al. 2009) have focused on individual sources of error and did not account for the impact of spatial and temporal aggregation. The current work was primarily motivated by this deficiency. The overall guiding principle of this research was to increase the value of AVHRR NDVI data for Earth science research.

1.2. Background

1.2.1. Normalized Difference Vegetation Index (NDVI)

$$\text{NDVI} = \frac{(\text{NIR} - \text{RED})}{(\text{NIR} + \text{RED})}$$ --- Eq: 1-1

NDVI (Eq:1-1) was first suggested by Rouse et al., (1973) and is one of the earliest and most popular vegetation indices. It attempts to decrease the atmospheric and surface Bidirectional Reflectance Distribution Function (BRDF) effects by normalizing the difference between red and NIR by total radiation.

NDVI has been shown to have a linear relationship with fPAR, from which important Earth surface biophysical variables like LAI and NPP can be derived (Myneni et al. 1997b; Prince and Goward 1995; Tucker 1979). This correlation is strongest when a vegetation canopy is neither dense nor sparse. When vegetation cover is too sparse, the background signal (e.g., soil color/moisture) can change

NDVI significantly (Huete and Jackson 1987). However, when vegetation cover is too dense, NDVI starts to saturate at LAI ≥ 2 and no longer correlates well with one widely-used aspect of the surface vegetation condition, that is LAI (Hatfield et al. 1985).

Variations in atmospheric composition (in particular aerosols and water vapor) affect the satellite based NDVI measurements significantly. Presence of atmospheric aerosols increases red reflectance, which in turn decreases NDVI. In AVHRR sensors, the broad spectral response functions the presence of atmospheric water vapor also decrease NDVI by causing a decrease in NIR reflectance (El Saleous et al. 2000). Presence of sub-pixel or thin cirrus clouds are difficult to detect and can also significantly contaminate NDVI measurements of vegetation and lead to misinterpretations. Surface and atmospheric BRDF is another source of error in NDVI signal (El Saleous et al. 2000; Kaufmann et al. 2000). For these reasons, use of satellite based NDVI data requires greater caution than is generally the case.

1.2.2. AVHRR Sensor

The AVHRR was designed in the mid 1970s for meteorological purposes. From 1978 onwards three versions of AVHRR instrument have been flown on the NOAA series of polar-orbiting satellite systems (Kidwell 1998). The first version of AVHRR instrument, which had a four band configuration, was carried on the TIROS-N satellite platform (launched October 1978). This was subsequently improved to a five-channel instrument (AVHRR/2) that was initially carried on NOAA-7 (launched June 1981). The latest version is a six channel instrument (AVHRR/3), which was

first carried on the NOAA-15 satellite platform launched in May 1998 (Robel 2007). Of these three versions, data from the AVHRR/2 and AVHRR/3 instruments are extensively used by the Earth system science community.

In the AVHRR/2 configuration, the AVHRR instruments collect data in a red (0.58–0.68 μm), a NIR (0.725–1.10 μm), a mid-infrared (3.55–3.93 μm) and two thermal (10.5–11.3 μm & 11.5–12.5 μm) spectral channels. Starting with the AVHRR/3 the sensor operation alternated between bands centered on 1.6 μm (channel 3a) during the day and on 3.75 μm (channel 3b) at night, unfortunately disrupting continuity of the channel 3 data, but the historical configuration returned in May 2003 when NOAA-16 again operated channel 3b continuously (Robel 2007).

In addition, the AVHRR/3 instruments allow improved low energy/light detection by incorporation of dual gain sensor characteristics for visible and NIR channels. The first half of the dynamic range of an AVHRR/3 channel represents 0 to 25% of the maximum detectible radiance at sensor, while the remaining 75% is represented by the second half of the dynamic range (Heidinger et al. 2002).
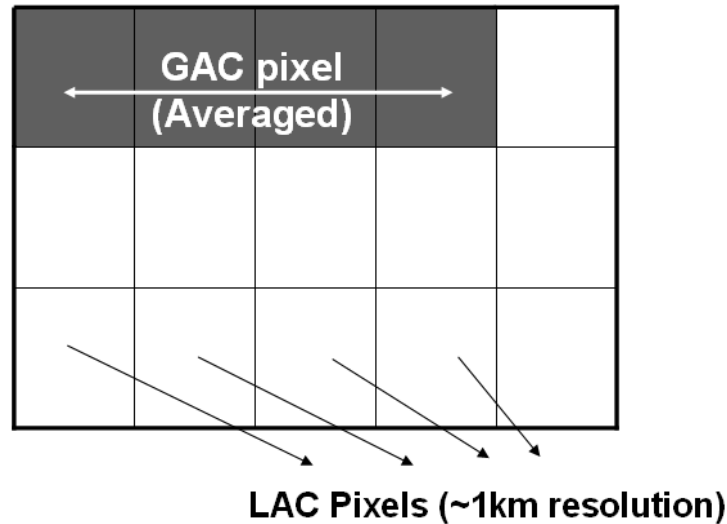
Fig. 1-1: *NOAA AVHRR Global Area Coverage (GAC) data are generated by averaging four out of every five samples (LAC pixels) along every third scan-line.*

The spatial resolution of the AVHRR data is approximately 1.1 km (~0.01° Local Area Coverage (LAC) data at nadir. Due to onboard resource limitations, the processor on board the satellite samples the real-time AVHRR data to produce the reduced resolution Global Area Coverage (GAC) data. GAC data are generated by averaging four out of every five samples (LAC pixels) along every third scan-line (Fig. 1-1). Although, the resultant data are treated as 4 km resolution, the actual spatial resolution of a GAC data pixel is 1.1x4.4 km with a gap of 3.3 km between the scan lines (Kidwell 1998). The 10-bit radiometric precision of the AVHRR data is retained.

1.2.3. Critical Aspects of Data from AVHRR Instruments

For long-term monitoring of land surface biophysical variables, it is essential that the data are well calibrated and exhibit a consistent dynamic range throughout the time series. However, AVHRR instruments lack onboard calibration for both red and NIR channels, the data is inherently difficult to correct for atmospheric interference (El Saleous et al. 2000), and the systematic changes in sun-sensor geometry due to satellite orbital drift (temporal precession of the equatorial crossing-time) add additional difficulty for the data users.

1.2.3.1. Sensor Degradation

The sensor calibration process relates radiometer response of the instrument to incoming radiation flux. The AVHRR instruments are thoroughly calibrated only before satellite launch. Past studies have shown that the calibration coefficients of reflectance channels change abruptly after launch and then continue changing slowly throughout the lifetime of satellites. These changes have generally been attributed to changes in sensor response as well as distortion of the spectral response function due to sensor degradation. The lack of onboard calibration to monitor these changes makes post-launch vicarious calibration mandatory and needs to be continuously updated (Abel et al. 1993; Gorman and McGregor 1994; Gutman 1999; Heidinger et al. 2002; Holben et al. 1990; Rao and Chen 1995; Rao and Chen 1996; Teillet et al. 1990; Vermote and Kaufman 1995).

Typically, the AVHRR reflectance data are calibrated by observing a time series of AVHRR data over radiometrically stable targets of known reflectance. For

example, many scientists have used observations over desert sites (Heidinger et al. 2002; Rao and Chen 1995; Rao and Chen 1996). Kaufman and Holben (1993) utilized atmospheric scattering and sun-glint over the ocean in addition to desert reflectance measurements for calibration of AVHRR reflectance data. Loeb (1997) utilized observations over snow/ice covered Polar Regions. Vermote and Kaufman (1995) used ocean observations to track the degradation of channel 1 and observations of clouds to monitor the changes in the channel 1/channel 2 ratio.

However, the accuracy of these vicarious calibration techniques is limited by the necessary assumptions employed, which include assumptions about the atmospheric conditions, surface BRDF and natural seasonal variability of the so-called stable target. The calibration accuracy achieved by these approaches is not better than 5% (Vermote and Saleous 2006a).

A much improved calibration technique is presented by El Saleous, (2000). This method estimates the offsets for calibration equations of AVHRR reflectance channels by averaging the deep space measurements available in each scan line, while the gains of the calibration equations are estimated using the in-flight calibration method, presented in Vermote and Kaufman (1995). Additional, ancillary datasets including detailed atmospheric composition information, wind speed, and reliable cloud detection algorithms are used to improve the performance of in-flight calibration method. This method has a demonstrated calibration accuracy of 1% (El Saleous et al. 2000; Pedelty et al. 2007; Vermote and Saleous 2006a).

The presence of dual-gain reflectance channels on the current series of AVHRR sensors (AVHRR/3 instruments) complicates the calibration processes

considerably. Heidinger et al., (2002) and Vermote et al., (2006) have presented calibration methods that use data from Moderate Resolution Imaging Spectrometer (MODIS) instruments for calibration of the AVHRR dual-gain reflectance channels (accuracy = 1%).

1.2.3.2. Orbital Drift

TIROS-N satellites which carry the AVHRR instruments are deployed on sun synchronous orbits. However, these sensor platforms suffer temporal recession of the equatorial crossing-time as each platform ages (Privette et al. 1995). This phenomenon is commonly known as orbital drift. Solar zenith angle (SZA) differences due to orbital drift are greatest near lower latitudes and steadily decrease with increase in latitude. For example, by year 1999, SZA at equator for the NOAA-14 AVHRR instrument deviated more than 35° from the angle at launch sun-sensor geometry. However, at 60° latitude, owing to increase in the number of satellite overpasses per day at high latitudes the change in SZA was only ~5° (Privette et al. 1995).

Surface BRDF and variation of atmospheric path length due to change in SZA makes NDVI sensitive to the orbital drift (El Saleous et al. 2000; Los et al. 2005; Sellers et al. 1996; Tanre et al. 1992). At the top of the canopy (TOC), NDVI increases with increase in solar zenith angle (Deering et al. 1992). This is due to increase in the fraction of solar radiation intercepted by the vegetation canopy. Past studies have shown that sensitivity of TOC NDVI to changes in SZA decreases with increase in LAI (Kaufmann et al. 2000).

Conversely, when considering the top of the atmosphere (TOA), an increase in SZA leads to a decrease in NDVI. This is due to the increase in atmospheric path length, which leads to an increase in path radiance in red and a decrease in NIR due to atmospheric absorption (Holben 1986; Privette et al. 1995; Tanre et al. 1992). The sensitivity of TOA NDVI to orbital drift increases with increase in LAI. This is because increase in LAI leads to reduced red reflectance, while the atmospheric contribution to the at-sensor red channel measurement (path radiance) increases with increase of SZA. Because NDVI is highly sensitive to red reflectance, orbital drift alone can cause considerable decrease in NDVI estimates. This atmospheric component of the impact of orbital drift on AVHRR-NDVI time series data is commonly observed at dense tropical forest sites (Tucker et al. 2005). Because, the impact of orbital drift on NDVI is systematic, it limits the investigation of temporal and spatial trends in land surface NDVI.

A number of empirical and statistical techniques have been used to deal with the impact of orbital drift. For example, Sellers et al., (1996) uses a simple empirical procedure, where straightforward empirical relationships between AVHRR NDVI and SZA were developed for dense green vegetation and bare soil land cover. These two relationships were then used to normalize the data to at nadir illumination condition by assuming a linear relationship between SZA correction and NDVI magnitude (Sellers et al. 1996). Jiang et al., (2008) dealt with the impact of orbital drift in Global Vegetation Index (GVI-2) dataset by adjusting the NDVI values to same level as NDVI data from the year of satellite launch. Pinzon et al., (2005) used an adaptive empirical mode decomposition (EMD) method to statistically remove the impact of

solar zenith angle drift in GIMMS NDVI dataset (Tucker et al. 2005). Several past studies have proposed orbital drift correction by systematic BRDF normalization using semi-empirical kernel models (Latifovic et al. 2003; Los et al. 2005; Privette et al. 1997; Roujean et al. 1992). Most of these studies have derived BRDF kernel parameters from AVHRR data themselves, even though most of the AVHRR datasets have incomplete atmospheric correction and inaccurate cloud masks. To overcome this shortcoming, Bacour et al., (2006) used POLDER data to parameterize BRDF kernels, but this method needed an *a priori* knowledge of existing land cover.

1.2.3.3. Atmospheric Correction

Atmospheric scattering and absorption substantially affect the AVHRR reflectance channels. The red and NIR channels are spectrally broad and include ozone and water vapor absorption bands. The channel 1 (red) encompasses an ozone absorption band and a weak water vapor absorption band. The channel 2 (NIR) contains a strong water vapor absorption band extending from 0.930 to 1.000 μm (Fig. 1-2) (Tanre et al. 1992; van Leeuwen et al. 1999). Because of this, the visible and near-infrared radiation reaching the satellite is differentially absorbed by atmospheric gases. Molecular backscatter by atmospheric aerosols introduces an additional directional reflectance (path radiance), which has high temporal as well as spatial variability (El Saleous et al. 2000; Tanre et al. 1992).
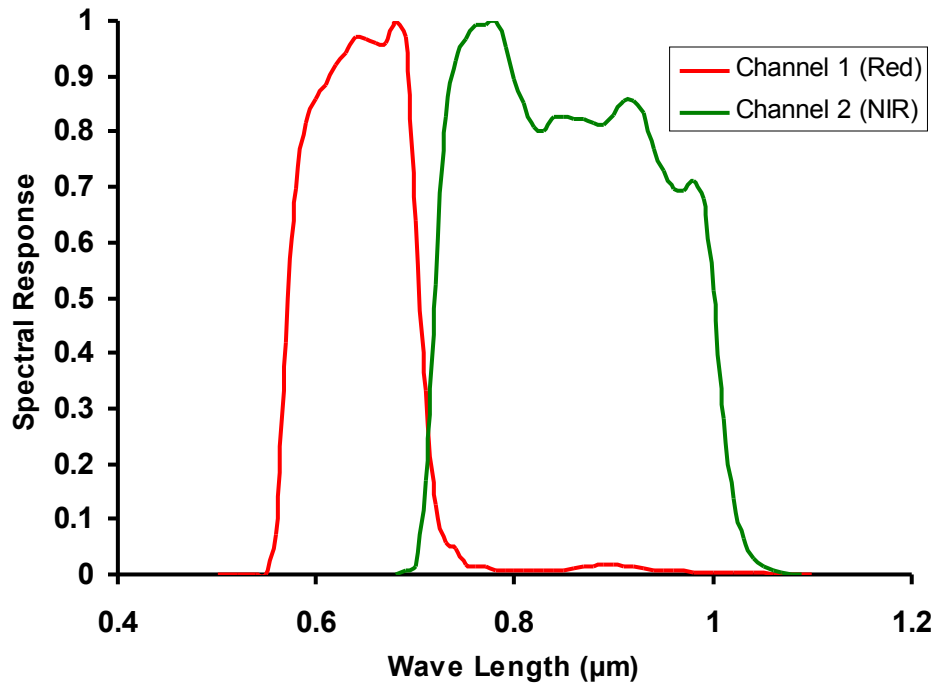
Fig. 1-2: *AVHRR NOAA-14 spectral response function*

Water vapor absorption can cause a 10-30% reduction of reflectance in NIR channel, while ozone absorption can reduce red channel reflectance by 5-15%, while atmospheric molecular scattering (Raleigh scattering) and aerosol effects can increase red channel reflectance as much as the reflectance of vegetated surfaces. During dense haze, path radiance can completely obscure surface properties. In terms of NDVI, even moderate haze can decrease the true NDVI of a densely vegetated surface by as much as ~ 0.1 (Tanre et al. 1992).

Unlike MODIS, AVHRR instruments do not have additional spectral channels that allow derivation of information about atmospheric composition to be used for atmospheric correction. However, correction for Raleigh scattering, and ozone absorption can be performed easily and has been included in processing streams of

many publicly available AVHRR NDVI datasets (James and Kalluri 1994; Pedelty et al. 2007). Correction for water vapor absorption, which is crucial for obtaining reliable NDVI measurements over sparsely vegetated areas, has also been successfully implemented by El Saleous, (2000). The aerosol effect which is highly variable in both space and time domains is the most challenging factor to correct. Temporal compositing techniques, like maximum NDVI, are widely used to minimize the effect of atmospheric spectral attenuation (Cihlar et al. 1994; Holben 1986), but this technique is of limited use in daily or short compositing periods (El Saleous et al. 2000).

1.2.4. Publicly available processed AVHRR NDVI datasets

Most vegetation studies do not use NDVI data calculated from at-sensor measures (TOA) from individual overpasses, but use processed and composited datasets. Some examples of GAC data based global datasets are LTDR (Long Term Data Record) (Pedelty et al. 2007), PAL (Pathfinder AVHRR Land) (James and Kalluri 1994), GIMMS (Global Inventory Modeling and Mapping studies) (Tucker et al. 2005), GVI (Global Vegetation Index) (Gutman et al. 1995; Kogan and Zhu 2001), GEOCOMP by Canadian Centre for Remote Sensing (CCRS) and a dataset produced at Joint Research Center (JRC) in Italy (Malingreau and Belward 1994).

There are also LAC datasets at 1km resolution. For example, the global 1km resolution NDVI produced by USGS (Eidenshink and Faundeen 1994; Teillet et al. 2000), a regional 1km dataset for conterminous USA and Alaska (Eidenshink 2006;

Eidenshink 1992), a similar dataset produced by CCRS for the Northern USA (Latifovic et al. 2005), and pan European 1km AVHRR NDVI data produced by JRC in Italy (Swinnen et al. 2007). There are similar projects in many other regions such as South-Africa, UK, Sweden, and Australia..

Some of these datasets are partially corrected for atmospheric perturbation and may omit extreme view zenith angles. Most of these datasets also use some kind of spatiotemporal aggregation, such as temporal maximum value compositing, and spatiotemporal smoothing. These corrections and aggregation techniques are generally acknowledged to decrease uncertainty in the satellite measurements of surface properties (Cihlar et al. 1998; Holben 1986). Table 1-1 presents a summary of dataset characteristics for some commonly used AVHRR NDVI datasets. Of these datasets, GIMMS dataset is currently the most popular while the relatively new LTDR dataset has the most comprehensive processing to date. These two datasets are discussed in more detail below.

Name of dataset	LTDR V3	PAL	GIMMS-G	GVI	USGS	USGS global
Spatial Extent	Global	Global	Global	Global	Conterminous USA and Alaska	Global
Spatial Resolution	0.05 degree (5km)	8 km	8 km	16 km	1km	1, 2, 4, 8, 16 km
Temporal Compositing period	Daily	10 day & monthly	bimonthly	weekly & monthly	weekly & biweekly	10day
Availability	1981- 2006	1981-2000	1981-2006	1985-2000	1989-present	06/1992 to 09/1993 and 02/1995 to 05/1996
Calibration	(Vermote and Kaufman 1995; Vermote and Saleous 2006b)	(Rao and Chen 1996)	(Los 1998; Rao and Chen 1996)	(Rao and Chen 1996)	(Heidinger et al. 2002; Teillet and Holben 1994; Vermote and Kaufman 1995)	(Teillet et al. 1990; Vermote and Kaufman 1995)
Cloud Screening	Red thresholds from MODIS global surface reflectance database	CLAVR (Stowe et al. 1995)	Temperature thrusholds for channel 5	No	CLAVR (Stowe et al. 1995)	no
Raleigh correction	Yes	Yes	No	No	Yes	Yes
Ozone correction	Yes	Yes	No	No	Yes	Yes
Water Vapor correction	Yes	No	No	No	Yes	No
Atmospheric Aerosol correction	Expected in next version	No	No (corrected for volcanic aerosols) (Vermote and Saleous 1997)	No	No	No
Data Input	GAC (Global Area Coverage)	GAC	GAC	GAC	LAC (Local Area Coverage)	LAC
Orbital Drift	Yes BRDF correction (Vermote et. 2009)	No	Yes Statistical time-series adjustment (Pinzon et al. 2002)	No	No	No
Key Citation	(Pedelty et al. 2007)	(James and Kalluri 1994)	(Tucker et al. 2005)	(Kidwell 1994, 1997)	(Eidenshink 2006; Eidenshink 1992)	(Eidenshink and Faundeen 1994; Teillet et al. 2000)

Table 1-1. *Summary of dataset characteristics for some AVHRR NDVI datasets*

1.2.4.1. Long-Term Data Record (LTDR)

LTDR is a consistent, long term dataset based on the AVHRR and MODIS data. LTDR is processed from AVHRR GAC data. The product includes daily NDVI as well as surface reflectance and radiance data at a spatial resolution of 0.05° (~5km at equator), which matches the Climate Modeling Grid (CMG).

The LTDR processing includes vicarious calibration of the visible and NIR channels using a cloud/ocean technique, which has been shown to have 1% error (Vermote and Kaufman 1995; Vermote and Saleous 2006b). The Earth location of each sensor measurement is mapped using inverse navigation technique (Rosborough et al. 1994). Unlike, forward navigation method, this technique does not lead to data gaps and geophysical bias (El Saleous et al. 2000). The atmospheric correction includes removal of the effects of Raleigh scattering, ozone, and water vapor. Ancillary data for water vapor and ozone correction were acquired from the NOAA Center for Environmental Prediction (NCEP) and Total Ozone Mapping Spectrometer (TOMS) respectively. An aerosol correction for this dataset is still being implemented (Pedelty et al. 2007) and not yet available in this version (LTDR version 3).

The LTDR version 3 data are normalized to a uniform sun-sensor geometry using the BRDF correction technique developed for MODIS data (Vermote et al. 2009a). This BRDF correction technique will be discussed in detail in chapter 3 of this dissertation. This version of the dataset also uses an improved cloud masking technique based on monthly thresholds for BRDF corrected visible channel. The global maps of visible channel thresholds are calculated from monthly mean and standard deviation of BRDF corrected (Vermote et al. 2009a) MODIS Terra and Aqua

data at CMG resolution of 0.05 degrees (Vermote et al. 2009b). The dataset is available in non-composited daily format with detailed ancillary data. This allows the data users to choose the appropriate compositing technique suitable to their application. The characteristics of some commonly used compositing methods are presented in chapter 4.

1.2.4.2. Global Inventory Modeling and Mapping studies (GIMMS)

GIMMS-g (Global Inventory Modeling and Mapping Studies) NDVI data are currently the most commonly used AVHRR NDVI data for time series analysis. Like LTDR, GIMMS data are also derived from GAC data. The GIMMS data processing includes calibration, corrections for orbital drift, corrections for volcanic aerosols, and spatiotemporal smoothing for removal of non-vegetation signal to produce bimonthly Maximum Value Composite (MVC) NDVI data. The data are currently (2010) available for years 1981 to 2006 (Tucker et al. 2005).

The GIMMS dataset also uses inverse navigation to map Earth location to each sensor measurement (El Saleous et al. 2000). Each composite image is further checked for navigation accuracy manually by comparing with a reference continental coastline map. Images with navigation errors greater than one pixel are investigated further, reprocessed and manually registered to the reference data.

The red and NIR channel data from NOAA-7 to 14 are calibrated using coefficients from Vermote and Kaufman (1995). The resulting NDVI fields are further adjusted using desert calibration technique from Los (1998). The data are then corrected for the effects of solar zenith angle drift using a statistical method (EMD)

described in Pinzon (2005). However, the GIMMS NDVI data derived from NOAA-16 uses preflight coefficients for calibration of red and NIR channels to produce bimonthly NDVI composites. The EMD method is then used directly to ensure zero inter-annual slopes at desert sites and also to adjust for the impact of solar zenith angle drift. The NOAA-16 NDVI data are then inter-calibrated to NOAA-14 data using SPOT Vegetation NDVI time series data (Tucker et al. 2005). The dynamic range of the entire NDVI dataset is further adjusted using non-linear regression equations to make it compatible with NDVI data from the MODIS and SPOT VEGETATION instruments (Tucker et al. 2005).

The GIMMS dataset does not employ any atmospheric correction except during the El Chichon and Mt. Pinatubo volcanic stratospheric aerosol periods (Vermote and Saleous 1997) and relies solely on bimonthly maximum value compositing technique to reduce the impact of atmospheric variations. Cloud screening is performed by a channel 5 thermal mask of 0° C for all continents and a 10° C mask for Africa.

1.2.5. Uncertainty in Remotely Sensed Quantitative Data

The outcome of any quantitative measurement depends not only on the item being measured, but also on the measuring system, the procedure, the operator, the environment and many other sources (Bell 1999). Thus, all measurements have associated uncertainties which reflect incompleteness in knowledge of the quantity being measured and have probabilistic basis.

18

Uncertainty in remotely sensed data is assessed by the validation process. The accepted definition of validation in Earth observation context is: assessment of the quality of the data by independent means (Justice et al. 2000). The satellite-based remotely sensed data products are usually validated by comparison with similar products derived from independent sources. These independent products are derived from a combination of in situ data and imagery from airborne and satellite based sensors.

For the validation process to be valid, the accuracy of the independent data product (reference data) has to be traceable to some known standard or, at minimum, it should be stable, consistent, and considerably more accurate than the signal that is being evaluated (Justice et al. 2000; Morisette et al. 2002).

To facilitate this activity an extensive network of validation sites called Earth Observation System (EOS) Land Validation Core Sites has been established at both regional and global scale (Morisette et al. 2002). This network adds to existing field programs like the LTER (Long Term Ecological Research) network (Franklin et al. 1990), science data networks like FLUXNET (Baldocchi et al. 2001), and AERONET (AErosol RObotic NETwork) (Holben et al. 2001) and international research efforts like the Southern Africa Fire and Atmosphere Research Initiative 2000 (SAFARI 2000) (Swap et al. 2000), and the Committee on Earth Observing Satellites (CEOS) working group on Calibration and Validation (WGCV) (Justice et al. 2000).

The MODIS Land data products validation process makes extensive use of data from these networks to derive reference data. One of the primary difficulties in using in situ data for validation is the scaling (aggregation) of the point data from

validation sites to the coarser spatial resolution of remotely sensed global or regional datasets (Morisette et al. 2002). This difference in scale is resolved by coupling field data with airborne data from sources like MODIS Airborne Simulator (MAS), the Airborne Visible Infrared Imaging Spectrometer (AVIRIS), and MODIS Quick Airborne Looks (MQUALS) and higher resolution satellite imagery data from instruments like IKONOS, Advanced Spaceborne Thermal Emission and Reflection Radiometer (ASTER), and Landsat (Morisette et al. 2002).

1.2.6. Past Studies on uncertainty in AVHRR NDVI data

AVHRR, unlike MODIS has not been subjected to such a rigorous validation process. Past studies of uncertainty in AVHRR reflectance and NDVI datasets have used various methodologies such as comparison with improved data from the same (Goward et al. 1993) or other sensors, validation using in situ data (Fensholt and Sandholt 2005), analysis of variation of the measurements for assumed stable targets (Cihlar et al. 1998) and use of spatial statistical methods such as semivariograms (Eklundh 1995). The AVHRR data have often been evaluated by comparison with better processed data from other sensors, for example Fensholt et al. (2006) who evaluated GIMMS and PAL AVHRR NDVI datasets by comparing them to data from SPOT, and Gallo et al. (2005) who compared AVHRR NDVI data with MODIS and investigated the feasibility of attaining continuity of NDVI products through future sensors systems.

Most of the past investigations of uncertainty in AVHRR reflectance and NDVI data have not been comprehensive either in scope or scale. They have mostly

focused on specific aspects of the uncertainty and their results are relevant to specific sites or regions only. For example, the study presented by Stellmes et al. (2010) evaluated NDVI trends in AVHRR data by comparing them to trends in Landsat data. The relevance of results from this study is limited to parts of Mediterranean. Fensholt et al., (2005) evaluated vegetation indices from AVHRR and MODIS instruments using 2 years of in situ data in Senegal. Fensholt et al., (2006) investigated how well AVHRR NDVI data from GIMMS and PAL datasets correlate with SPOT data in African continent. Gallo et al., (2005) similarly investigated the strength of correlation between AVHRR and MODIS data in the conterminous United States. Numerous other examples also exist in recent literature (Brown et al. 2006; Cihlar et al. 1998; Eklundh 1995; Fensholt et al. 2009; Goward et al. 1993; Ji et al. 2008; Kangas et al. 2001; Ouaidrari et al. 2003; Pouliot et al. 2010). Because many influential studies in the field of Earth system science have been based on AVHRR NDVI, a thorough understanding of uncertainty is long overdue.

1.2.7. Precision Assumed for AVHRR NDVI data

The approximate precision of NDVI of terrestrial vegetation is often, implicitly, assumed to be between ~0.03 and ~0.08 NDVI units. For example Jia et al., (2003) reported changes in the vegetation of arctic Alaska over 21 years using AVHRR data of 0.056±0.0032 to 0.082±0.028 NDVI units. Slayback et al., (2003) reported an increase of 0.027 to 0.081 NDVI units for a period of 18 years (1982-99) for global latitude bands from 35° to 75° N. Piao et al., (2003) reported an increase of similar magnitude (0.0325 NDVI units) in 18 years in China. There are many other studies using AVHRR NDVI (Piao et al. 2006; Young and Harris 2005), where

changes much smaller than 0.03 units are treated as significant. At this time, the accuracy of the AVHRR data implied in these studies has not been validated and the significance of the differences is not stated explicitly. Thus, it is possible that some studies have assumed greater accuracy than is justified.

1.2.8. Statistical Framework for Estimation of Uncertainty in Remotely Sensed Data

The National Polar-orbiting Operational Environmental Satellite System (NPOESS) project has defined a statistical framework which represents uncertainty in two components: (1) systematic bias; and (2) random-error. Of these two, the random-error component represents relative error which is pertinent for inter-annual studies, while the information about systematic bias becomes relevant only when the data are being used in conjunction with other datasets. This study will primarily focus on random-error component of uncertainty (Fig. 1-3). To facilitate discussion the terms 'random-error' and 'uncertainty' will be used interchangeably in rest of this dissertation.
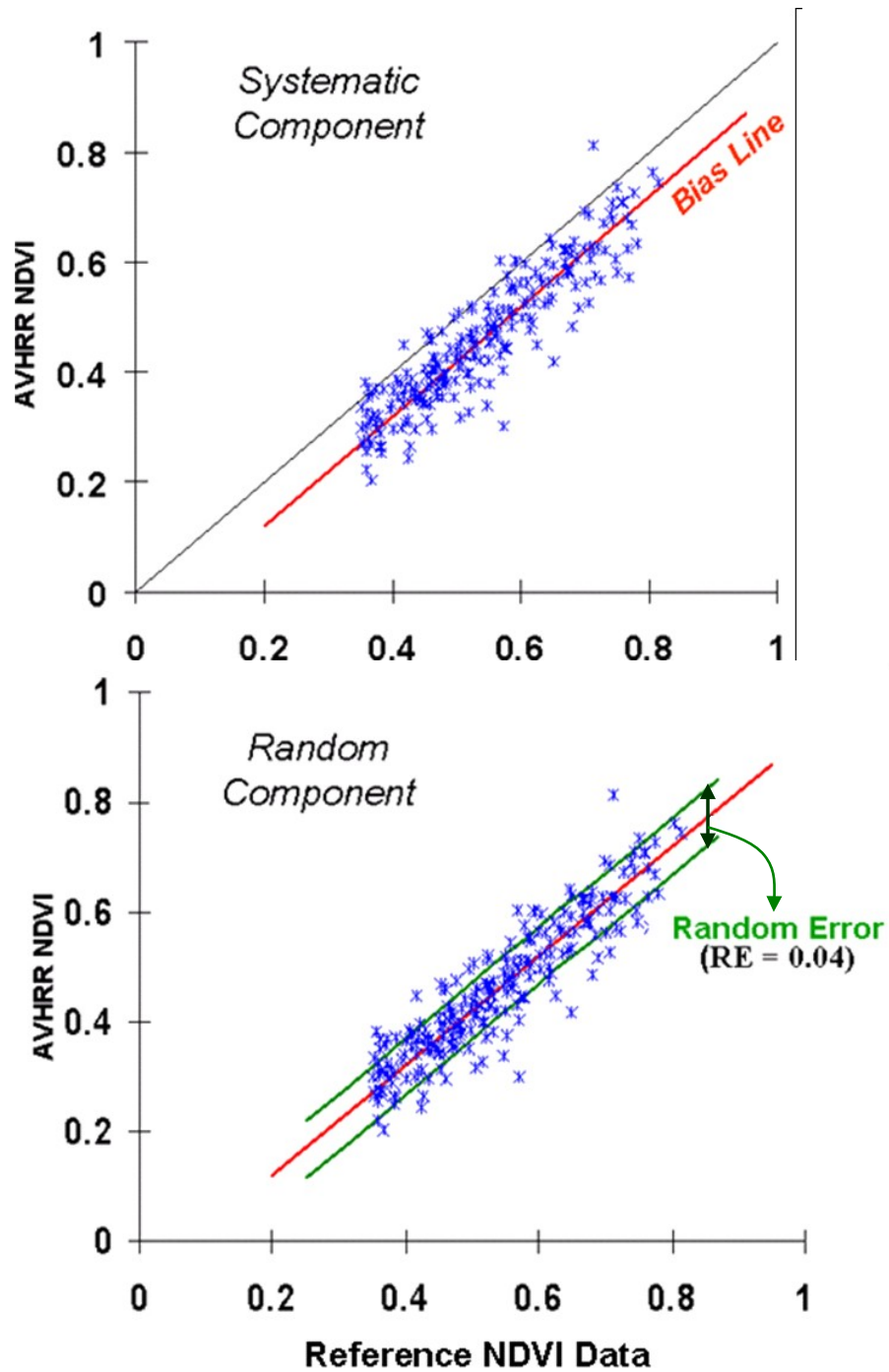
Fig. 1-3: *Statistical framework used for calculation of random-error.. This analysis used non-composited daily NDVI data from 2003 to 2006.*

Analysis presented in Fig. 1-3 illustrates a statistical framework for estimation of the uncertainty (random-error) using growing season NDVI data from an agricultural site in southwestern Australia. Uncertainty here is calculated as the standard deviation of the data relative to the systematic-bias line. The systematic-bias line can be estimated using two methods: (1) by fitting a first order polynomial to the two dimensional scatter plot comparing AVHRR NDVI data to the reference data; (2) when the slope of the polynomial is one or the R-squared of the polynomial fit is too low the bias can be directly estimated as the mean of deviations of the AVHRR NDVI data from the reference data. The uncertainty of 0.04 estimated for LTDR AVHRR NDVI data at the example site in Fig. 1-3, implies that, at this site an NDVI value of 0.6 will actually have 68% probability of ranging between 0.56 and 0.64 (i.e. 0.6±0.04) and 95% probability of ranging from 0.52 to 0.68 (i.e. 0.06±0.08).

When evaluating satellite data using in situ measurements the presence of systematic-bias is not necessarily an evidence of error. Rather it could be a result of fundamental differences in sensor design (e.g., spectral response function, radiometric resolution, sensor calibration, etc.), atmospheric interference in satellite data, and shortcomings in the process of scaling up the point data to the coarser satellite resolution (Cohen and Justice 1999; Morisette et al. 2002). Random-error on the other hand can be attributed to measurement error, variations in atmospheric composition, residual cloud contamination, geolocation error, and surface and atmospheric BRDF effects in satellite data.

When evaluating a satellite based remotely sensed dataset using a higher quality satellite based dataset, the systematic-bias is a result of differences in sensor design

and deployment, such as spatial resolution, spectral response function, sensor
calibration, radiometric resolution, sun-sensor geometry, and differences in post-
processing algorithms (atmospheric correction, BRDF correction, and vicarious
calibration). The random-error can be attributed to the geolocation error, and variation
of pixel size in relation to viewing geometry, and the complex interactions of the
differences between the sensor systems. Clearly, for this method of evaluation to be
valid, the reference dataset has to have significantly lower error.

1.3. Research Goals and Dissertation Structure

Steps	Research	Chapters
Part 1	Investigation of errors due to atmospheric variation	Chapter 2
Part 2	Investigation of impact of orbital drift	Chapter 3
Part 3	Quantification of overall uncertainty and impact of spatial and temporal aggregation	Chapter 4

Table 1-2: *Flow of the research activities within the dissertation structure*

The overall goal of this research was to estimate uncertainty of AVHRR NDVI
data and the impact of various degrees of spatial and temporal aggregation. This was
achieved in 3 steps (Table 1-2). The first part investigated the extent of uncertainty
due to inadequate atmospheric correction in the three widely-used, publicly-available,
AVHRR NDVI datasets. The second part investigated the interaction between surface
and atmospheric BRDF and its contribution to the sensitivity of AVHRR-NDVI time
series data to orbital drift. A new approach for surface BRDF correction was
proposed. The third part focused on estimation of spatially-explicit, comprehensive
uncertainty metrics for AVHRR NDVI data and the impact of various degrees and
types of temporal and spatial aggregation. This part primarily focused on the LTDR

dataset. The overall guiding principle of the investigation was to provide detailed information about the precision of AVHRR NDVI data and the corrections that can increase the value of the data for Earth science research.

This dissertation consists of 5 chapters. The Chapters 2, 3, and 4 are presented in the self-contained format of journal articles (one of which is published and one in review) and present results from parts 1, 2, and 3 of this dissertation respectively (Table 1-2). Chapter 5 summaries the results and discusses their implications on Earth system science studies.

Chapter 2: Investigation of Errors Due to Atmospheric Composition

2.1. Introduction

Most of the available AVHRR NDVI datasets have incomplete atmospheric correction, resulting in considerable, but largely unknown, uncertainty in the significance of differences in NDVI and other short wave observations from AVHRR instruments. The purpose of this study was to gain a better understanding of the impact of this incomplete or absent atmospheric correction in widely-used, publicly available processed AVHRR-NDVI long-term datasets.

Three datasets were evaluated: TOA; PAL; and an early version of the new Long Term Data Record (LTDR) (http://ltdr.nascom.nasa.gov/ltdr/ltdr.html) (Pedelty et al. 2007). The other publicly available datasets like GIMMS and GVI have no atmospheric correction and rely solely on temporal compositing to reduce the effects of changes in atmospheric properties. Uncertainty was assessed by comparing the processed AVHRR datasets to atmospherically corrected AVHRR data at AERONET sites and analyzing simulated AVHRR NDVI data.

2.2. Data and Methods

2.2.1. Approach

The extent of uncertainty due to inadequate atmospheric correction in the widely used AVHRR NDVI datasets was investigated by comparison with data to

which comprehensive atmospheric correction has been applied. Atmospheric compositions derived from AERONET sunphotometer data were used for space and time-specific atmospheric correction. These corrected data are referred to as reference data. The statistical framework presented in chapter 1 (section 1.2.8) was used to estimate uncertainty metrics.

AERONET is an aerosol monitoring system and part of the extensive remote sensing validation networks established in recent years over a wide variety of land cover types and latitudinal zones. AERONET is a world-wide network of automatic sun and sky scanning spectral radiometers which measure every 15 min. The data from these instruments are processed to derive atmospheric aerosol optical properties, precipitable water, and aerosol size distribution (Holben et al. 2001). In 1999, there were about 100 operational sites and by 2006, the network had grown to more than 300.

This study evaluated TOA (no atmospheric correction) (Pedelty et al. 2007), PAL, and LTDR datasets. The PAL processing stream includes correction for Raleigh scattering and ozone, while the early version of LTDR that was tested here is corrected for Rayleigh scattering, ozone, and atmospheric water vapor (Pedelty et al. 2007). PAL data were resampled from 8km to 5km resolution using nearest neighbor method to make them comparable to LTDR and TOA data with 5km (0.05°) resolution. The year 1999 was used for this investigation because non-composited, individual, satellite overpass data were available for all three datasets used (TOA, PAL, and LTDR) and there were an adequate number of operational AERONET sites.

Although the data from year 1999 provided a useful overview of the error patterns in AVHRR NDVI data record, it represented only one year and most of the data were in North America and in semi-arid and desert areas elsewhere, owing to the smaller network of AERONET stations at that time. Moreover, aggressive cloud masking derived from AERONET led to very few data being available to investigate the impacts of temporal compositing. To overcome these shortcomings, further analysis was performed on simulated AVHRR data for representative sites in tropical forest (Belterra, Brazil), savanna (Skukuza, South Africa), and semi-arid (Sevilleta, Arizona, USA).. This was done by using atmospheric conditions and cloud cover frequency from AERONET, NDVI phenology derived from MODIS, and sun-target-sensor geometry from the full length (1981-2000) of the AVHRR data record.

2.2.2. Reference Data

Comprehensive atmospheric correction was carried out on TOA AVHRR data for 9 pixel matrices centered on each available AERONET site (Fig. 2-1) using the 6S (Vermote et al. 1997) atmospheric radiative transfer program. Aerosol optical thickness, aerosol size distribution, and precipitable water data from AERONET as well as ozone concentration data from TOMS (Total Ozone Mapping Spectrometer) (McPeters and Labow 1996) were utilized in this atmospheric correction process. The TOMS instruments measure ultraviolet (UV) radiation backscattered by Earth's atmosphere and surface at wavelengths between 310 - 380 nm. UV wavelengths shorter than 340 nm are used to estimate ozone concentration in the atmospheric column.
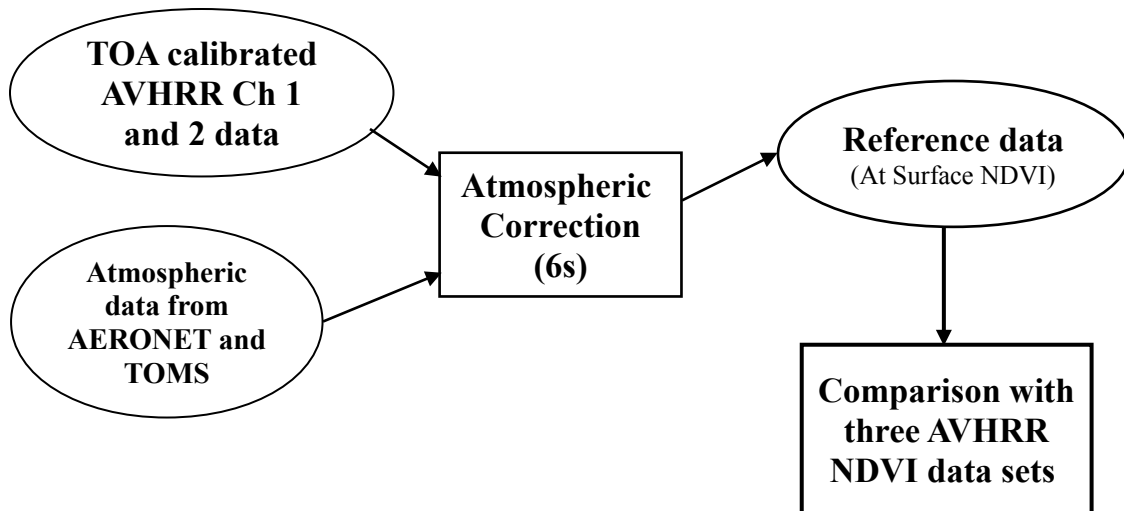
Fig. 2-1: *Schematic view of the data processing for reference data*

Only AVHRR pixels with view zenith angle less than 42° were used. The data were masked for cloud and cloud shadow using quality flags from LTDR (El Saleous et al. 2000; Stowe et al. 1995). Further cloud masking was performed using an aggressive AERONET derived cloud mask. After application of 6S to remove atmospheric effects from the reference data, the NDVI and surface reflectance were used to estimate the magnitude of the errors of the publicly-available, processed, AVHRR NDVI datasets. After masking for cloud and water, approximately 580 data points (sites x days) remained from 48 AERONET sites (Fig. 2-2). Of these data points 29% were clear (AOT < 0.05), 62% were average (AOT = 0.05 to 0.25), and 9% were hazy (AOT > 0.25). Most of these data points were in North America (60%) or in semi-arid (30%) and desert (17%) areas elsewhere (Fig. 2-2).
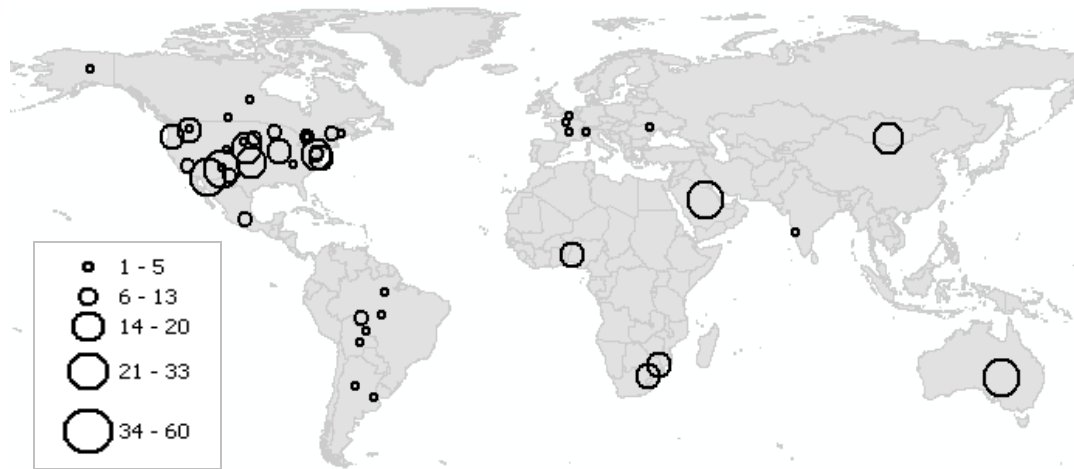
Fig. 2-2: *Spatial distribution of AERONET sites used to calculate reference data. After masking for cloud, cloud shadow, and view zenith angle greater than 42°, only 580 data points from 48 AERONET sites remained for use in calculation of the reference data. The number of data points is indicated by the diameter of the circle (see inset).*

2.2.3 Simulated AVHRR time series

6S radiative transfer program was used to create a 1981 to 2000 simulated time series for AERONET sites: Belterra (54.952° W, 2.649° S), Skukuza (31.588° E, 24.992° S), and Sevilleta (106.885° W, 34.355° N) to represent forest, savanna, and semi-arid land cover types respectively. Atmospheric composition and a cloud mask were derived from one representative year of AERONET measurements and TOMS. Representative phenology was derived from MODIS data. The sun-sensor-target geometry was extracted from LTDR data. Solar zenith angle and view zenith angles were constrained to less than 75° and 50° respectively.

At-surface reflectance measures derived from MODIS was first converted to TOA at-sensor measure using 6S. The calculated TOA reflectance data were then corrected for Raleigh scattering and atmospheric absorption using 6S to produce PAL type data. Further introduction of correction for water vapor simulated LTDR data.

2.3. Results and Discussion

Comparison of data from red and near infra-red channels of TOA, PAL and LTDR datasets with reference data at the AERONET stations (Table 2-1) showed that in both channel 1 and 2 LTDR has greatly improved systematic-bias and uncertainty when compared to PAL and TOA data. PAL consistently underestimated reflectance in both channels, which can be attributed to use of obsolete calibration and lack of water vapor correction. The comparison of the NDVI from these datasets with reference data shows that LTDR is closest (systematic-bias = -0.024, uncertainty =

0.037 for data points with average atmospheric conditions) followed by PAL (systematic-bias = -0.035, uncertainty = 0.068), and TOA (systematic-bias = -0.112, uncertainty = 0.0684) (Table 2-1).

Band	DATA	Clear (AOT < 0.05)		Average (AOT = 0.05 to 0.25)		Hazy (AOT > 0.25)	
		Systematic-bias	Uncertainty	Systematic-bias	Uncertainty	Systematic-bias	Uncertainty
CH1	TOA	-0.0020	0.0219	-0.0060	0.0265	-0.0120	0.0352
CH1	PAL	-0.0225	0.0228	-0.0189	0.0214	-0.0121	0.0409
CH1	LTDR	0.0005	0.0079	0.0032	0.0174	0.0152	0.0267
CH2	TOA	-0.0358	0.0261	-0.0425	0.0303	-0.0561	0.0286
CH2	PAL	-0.0508	0.0386	-0.0577	0.0366	-0.0786	0.0413
CH2	LTDR	-0.0002	0.0102	-0.0023	0.0182	0.0004	0.0212
NDVI	TOA	-0.0791	*0.0613*	-0.1120	*0.0684*	-0.1521	*0.1059*
NDVI	PAL	-0.0145	*0.0606*	-0.0352	*0.0418*	-0.1137	*0.0877*
NDVI	LTDR	-0.0064	*0.0206*	-0.0243	*0.0373*	-0.0612	*0.0780*

Table 2-1: *Systematic-bias and uncertainty for red channel (CH1), near infrared channel (CH2), and NDVI for TOA, PAL, and LTDR data. Of the 580 data points 168 (29%) were clear, 360 (62%) were average, and 52 (9%) were hazy.*

Simulated Data	Land cover	Clear (AOT < 0.05)		Average (AOT = 0.05 to 0.25)		Hazy (AOT > 0.25)	
		Systematic-bias	Uncertainty	Systematic-bias	Uncertainty	Systematic-bias	Uncertainty
TOA	semi-arid	-0.0616	0.0226	-0.0667	0.0234	-0.1400	0.0629
TOA	savanna	-0.1701	0.0436	-0.1770	0.0510	-0.3047	0.1816
TOA	forest	-0.2469	0.0821	-0.2804	0.0849	-0.5861	0.1880
PAL	semi-arid	-0.0393	0.0114	-0.0514	0.0155	-0.1323	0.0781
PAL	savanna	-0.0792	0.0154	-0.1072	0.0426	-0.2523	0.1711
PAL	forest	-0.0555	0.0263	-0.1242	0.0719	-0.5077	0.2185
LTDR	semi-arid	-0.0071	0.0610	-0.0109	0.0109	-0.0846	0.0850
LTDR	savanna	-0.0137	0.0105	-0.0379	0.0356	-0.1661	0.1641
LTDR	forest	-0.0252	0.0206	-0.0845	0.0611	-0.4291	0.1988

Table 2-2: *Systematic-bias, and Uncertainty for NDVI from simulated TOA, PAL, and LTDR datasets. For the forest site; 20 (4%), 376 (75%), and 105 (21%) of 501 data points had clear, average, and hazy atmospheres respectively. For the savanna site; 40 (9%), 317 (71%), and 89 (20%) of 446 data points had clear, average, and hazy atmosphere respectively. For the semi-arid site; 384 (52%), 348 (47%), and 8 (1%) of 740 data points had clear, average, and hazy atmosphere respectively.*

Land cover	Comp Period	Clear (AOT < 0.05)			Average (AOT = 0.05 to 0.25)			Hazy (AOT < 0.25)		
		Systematic-bias	Uncertainty	% data	Systematic-bias	Uncertainty	% data	Systematic-bias	Uncertainty	% data
Semi-arid	daily	-0.0611	0.0217	52	-0.0643	0.0214	47	-0.1400	0.0629	1
Semi-arid	10day	-0.0514	0.0191	55	-0.0541	0.0186	45	-	-	0
Semi-arid	15day	-0.0485	0.0174	58	-0.0514	0.0178	42	-	-	0
Semi-arid	monthly	-0.0447	0.0157	69	-0.0474	0.0197	31	-	-	0
Savanna	daily	-0.1614	0.0360	9	-0.1727	0.0470	71	-0.3067	0.2130	20
Savanna	10day	-0.1516	0.0316	11	-0.1594	0.0420	71	-0.3072	0.2158	18
Savanna	15day	-0.1499	0.0328	11	-0.1573	0.0426	72	-0.3026	0.2059	17
Savanna	monthly	-0.1487	0.0328	16	-0.1528	0.0416	72	-0.2552	0.1716	12
Forest	daily	-0.2347	0.0702	3	-0.2830	0.0774	72	-0.5241	0.1585	22
Forest	10day	-0.2179	0.0663	3	-0.2610	0.0754	75	-0.5223	0.1694	22
Forest	15day	-0.2075	0.0415	3	-0.2554	0.0722	77	-0.5428	0.1663	20
Forest	monthly	-0.1967	0.0302	4	-0.2434	0.0721	74	-0.5036	0.1401	22

Table 2-3: *Impact of temporal maximum value compositing (MVC) on Systematic-bias, and Uncertainty for simulated TOA NDVI time series data*

The error budget of simulated time series (Table 2-2) compares well with empirically derived error budget in Table 2-1. For the forest and savanna sites most of the data points (> 70%) had average atmospheric conditions (AOT = 0.05 to 0.25) and about 20% were hazy (AOT>0.25). However, for semi-arid site more than half data points had clear atmospheric conditions (AOT < 0.05) and only 0.5% points were hazy. Both the direct validation (Table 2-1) and site specific simulated error budget (Table 2-2) show that in hazy conditions all three datasets become very unreliable with uncertainty as high as 0.22 in the forest site. These results show uncertainty for TOA NDVI data ranged from 0.023 for clear atmospheric conditions at the semi-arid site to 0.085 for average atmospheric conditions at the forest site (not considering data points with hazy atmospheric conditions). For LTDR NDVI data uncertainty varied between 0.0061 for clear atmospheric conditions at semi-arid site to 0.0611 for average atmospheric conditions at forest site. A similar decrease in uncertainty was observed at the savanna site.

Usually AVHRR time series data are used in temporally composited format. Many methods are used for compositing, of which MVC (Maximum Value Composite) (Holben 1986) is most widely used. Various lengths of compositing periods are used. Table 2-3 shows the impact of simple temporal MVC on bias and uncertainty of TOA NDVI data at forest, savanna and semi-arid sites. From Table 2-3 it can be observed that there is no significant impact of temporal compositing on Uncertainty in all three sites in average as well as hazy atmospheric conditions. Most of the data points selected for savanna and forest sites with MVC criteria had average and hazy atmospheric conditions. It was also observed that various degrees of

compositing did not significantly change the proportion of data points in clear, average, and hazy atmosphere categories. This was due to persistent high aerosol content in atmosphere which limits the capacity of MVC method to find a clear day. This persistence of high aerosols is a common feature of these and similar sites. MVC was useful only in sites where high aerosol content persisted for shorter periods than the length of the composing period. Cloud frequency and high values of AOT play an important role in the effectiveness of MVC.

2.4. Conclusions

The results presented in the Tables 2-1 and 2-2 show that LTDR has the least errors followed by PAL, and TOA. Of the two metrics (systematic-bias, and uncertainty (random-error)) used to describe the errors; uncertainty, which represents standard deviation of the estimates adjusted for the mean bias is most pertinent for inter-annual studies as it represents random component of the error.

Although both PAL and LTDR data have lower error budget in both clear and average atmospheric conditions, it was observed that magnitude of bias and uncertainty is driven primarily by aerosol content in the atmosphere and its interaction with solar illumination angle and cloud frequency. It was also seen that temporal maximum value compositing technique does not cause significant improvement of the error budget in regions experiencing persistently high AOT due to, for example, biomass burning. Thus implementation of aerosol correction or at least some technique to identify and reject even MVCs that still have high aerosol contamination would greatly improve the error budget of the data records.

Spatiotemporal aggregation techniques, which are used extensively by NDVI data users, can decrease uncertainty but one has to be careful to account for the spatiotemporal autocorrelation. For example if a region is experiencing fairly uniform atmospheric conditions for extended periods of time, spatiotemporal aggregation will not decrease the impact of atmosphere on the data. Non-stationarity introduced in the data due to systematic intra-annual and inter-annual changes in sun-sensor-target geometry (orbital drift) also has to be considered. The next chapter will focus on the impact of orbital drift on long-term AVHRR NDVI time series data.

Chapter 3: Investigation of Impact of Orbital Drift on Long-Term AVHRR NDVI Time Series Data

3.1. Introduction

The NDVI time series data derived from AVHRR series of instruments suffer from significant variations as a result of the orbital drift of the satellites through their active lives. Orbital drift causes a systematic change in SZA. The sensitivity of AVHRR NDVI data to the SZA change depends on surface BRDF, atmospheric composition and the type of atmospheric correction used. The systematic error caused by orbital drift hinders the detection and interpretation of temporal Earth-surface vegetation dynamics.

The research presented in this chapter had two objectives. The first objective was to investigate the contributions of surface and atmospheric bidirectional effect to the impact of orbital drift on AVHRR-NDVI time series data. The second was to examine the effectiveness of MODIS based BRDF parameters (Vermote et al. 2009a) for remediation of the impact of orbital drift on AVHRR NDVI data.

3.2. Data and methods

3.2.1. Impact of Orbital Drift on AVHRR NDVI Time Series

The contribution of surface BRDF and atmosphere to the impact of orbital drift on AVHRR-NDVI time series data was investigated using simulated NDVI time

series data with varying degrees of vegetation cover (10%, 50%, and 95%); atmospheric composition (TOC; and TOA); and at different latitudes (0°, 30°, and 60°). These simulated time series data were created using actual sun sensor geometry for specific latitudes and 0° longitude. The temporal extent of the simulated data was restricted to the first 5 years (1995 to 1999) of NOAA-14 satellite's operational life. A constant AOT (Aerosol Optical Thickness) of 0.15 was assumed and view zenith angle (VZA), and SZA were restricted to values below 45°, and 75° respectively. Inter-annual and seasonal variations in vegetation and atmospheric conditions in the modeled time series were kept constant to facilitate examination of trends introduced by surface and atmospheric BRDF. Contributions of atmosphere and surface BRDF to the impact of orbital drift on AVHRR NDVI time series data were estimated using the 6S atmospheric radiative transfer program (Vermote et al. 1997) and the FLIGHT (Forest LIGHT) model (North 1996).

FLIGHT is a 3D canopy radiative transfer model which uses Monte Carlo simulation of photon transport to simulate light interaction in the forest canopy. The spatial discontinuity of the forest canopy is approximated using a hybrid approach. Geometric primitives (circle, ellipse, cylinder and cone) are used to define the structural elements (crowns and trunks) of the forest. Foliage is approximated within the crowns by foliage structural parameters (area density, angular distribution, and size) and optical properties of leaf and branch material. BRDF is estimated by simulation of the photon path and the chain of scattering events incurred by a photon during its journey from the source to the receiver or to its absorption within a forest representation. The photon path simulation is modified to reflect finite sized scatters

41

(Jupp and Strahler 1991). The model has been validated against field measurements and by inter-comparison with other three dimensional radiative transfer models (Pinty et al. 2004). Comparisons with ground (PARABOLA) and airborne (ASAS) data confirmed the ability of FLIGHT model to estimate BRDF and albedo for even the most complex case of open coniferous canopies (North et al. 1996; North 1996), with an error of 2% for bidirectional reflectance factors (BRF) and 0.5% for albedo.

3.2.2. Effectiveness of MODIS BRDF parameters for BRDF Correction of AVHRR NDVI Time Series Data

The effectiveness of the BRDF correction technique developed for MODIS data (Vermote et al. 2009a) in removing the impact of surface BRDF on the effects of orbital drift on AVHRR NDVI data was examined by applying this technique directly to modeled TOC NDVI time series data as well as actual AVHRR NDVI data from LTDR dataset (http://ltdr.nascom.nasa.gov/). Two sites, with different degrees of vegetation cover (50% and 95%), were used for this purpose (Fig. 3-1). The analysis was restricted to the data from first 5 years (1995 to 1999) of NOAA-14 satellite's operational 1 life. The VZA was restricted to less than 45° and solar zenith angle was restricted to less than 75°.

Fig. 3-1: *Aerial views of sites used for BRDF correction. Site 1 has 50% vegetation cover and is located in south-western Australia (116.167°E, 32.1944°S). Site 2, with 95% vegetation cover, is located in north-eastern Australia (145.8°E, 17.4°S).*

3.2.2.1. Study Sites

Of the two sites used in this study (Fig. 3-1), the first site (Site-1) is located in south-western Australia (116.167°E, 32.1944°S) and has 50% vegetation. Data from this site were used to illustrate the effectiveness of BRDF correction technique on sites expected to experience high impact of orbital drift on TOC NDVI. Site-2 has 95% vegetation cover, and is located in north-eastern Australia (145.8°E, 17.4°S). Data from this site were used to demonstrate the impact of BRDF correction on sites with minimal impact of orbital drift on TOC NDVI but prominent contribution of atmospheric BRDF. Both of these sites have evergreen vegetation and experience fairly low aerosol contamination. The rationale behind using only evergreen sites was to facilitate investigation of the impact of orbital drift alone on the inter-annual NDVI trends.

3.2.2.2. The MODIS BRDF Correction Technique

The MODIS BRDF correction technique presented by Vermote et al., (2009) assumes that the shape of the BRDF varies more slowly than the reflectance and this change is linearly related to NDVI. This relationship with NDVI is then used to account for seasonal variations in BRDF shape. A relationship between BRDF parameters and NDVI for each pixel is then derived from the full MODIS time series record. Because this method uses MODIS data for definition of BRDF shape, it is not limited by incomplete atmospheric correction and inaccurate cloud masks of AVHRR NDVI datasets.

The BRDF shape can be described by two parameters, R (surface scattering) and V (volume/canopy scattering). Assumption of a constant BRDF shape for the entire year allows an easy inversion of parameters R and V from MODIS data. These parameters can then be used for BRDF correction of reflectance the AVHRR time series data. MODIS directional reflectance time series data, when corrected using this method, showed considerable decrease in high frequency variability. However, vegetation structure generally has an annual phenological cycle of greening, growth, and senescence, which has a direct effect on the BRDF. Therefore, parameters V and R also vary with seasonal change in vegetation greenness (NDVI). Inclusion of this variation of V and R parameters in relation to NDVI in the BRDF correction process improved the correction of the MODIS time series data. A full description and discussion of this method can be found in Vermote et al., (2009).

3.2.2.3. Modeled AVHRR TOC reflectance data

Modeled AVHRR TOC reflectance data were calculated for these two sites using FLIGHT, which is capable of modeling the impact of extreme solar zenith angles on directional reflectance of a vegetated surface. For each site, the FLIGHT model was first parameterized using approximate forest structural values (percent forest cover, mean crown diameter, and mean canopy height) inferred from high resolution satellite imagery (Fig. 3-1). The foliage parameters (leaf area density, leaf angular distribution, and leaf size, and optical properties of leaf and branch, etc) were populated using default values provided by the FLIGHT model (Table 3-1). These parameters were then iteratively varied within a reasonable range to arrive at the red

45

and NIR BRDF shapes, representing the variation of reflectance in relation to VZA, similar to the ones produced by BRDF parameters from MODIS data (Vermote et al. 2009a) at a constant SZA of 45°. The goal was to create a realistic definition of forest vegetation structure in FLIGHT model to facilitate the investigation of impact of extreme SZA variations present in AVHRR datasets.

FLIGHT Parameters	Site-1	Site-2
% Vegetation cover	50	95
Crown diameter/height	1	1
Total canopy height	10 m	55 m
Scene LAI	2	6
Leaf red reflectance	0.07	0.045
Leaf NIR reflectance	0.45	0.5
Leaf red transmittance	0.015	0.02
Leaf NIR transmittance	0.39	0.4
Bark red reflectance	0.23	0.1
Background NIR reflectance	0.21	0.5

Table 3-1*: Vegetation structural and optical information used to parameterize the flight model for forests at two sites depicted in Fig. 3-1.*

This study also utilized AVHRR data from the LTDR version-2 dataset. The product includes daily surface reflectance and NDVI products at a resolution of 0.05°. This version includes atmospheric corrections for Rayleigh scattering, ozone, and water vapor. Aerosol correction is still being implemented (Pedelty et al. 2007).

3.3. Results and Discussion

3.3.1. Impact of Orbital Drift on AVHRR NDVI Time Series

The impact of vegetation cover on the relationship between TOC-NDVI and SZA presented in Fig. 3-2 indicated that the magnitude of TOC NDVI increased with an increase in SZA. It was also observed that the NDVI times-series data at sites with 95% and 10% vegetation cover showed a lesser impact of SZA change when compared to the site with 50% vegetation cover. The rate of change of NDVI per 10° SZA was 0.070 for the site with 50% vegetation cover, while at sites with 10%, and 95% vegetation cover the rate of change of NDVI was only 0.013, and 0.008 NDVI units per 10° SZA.
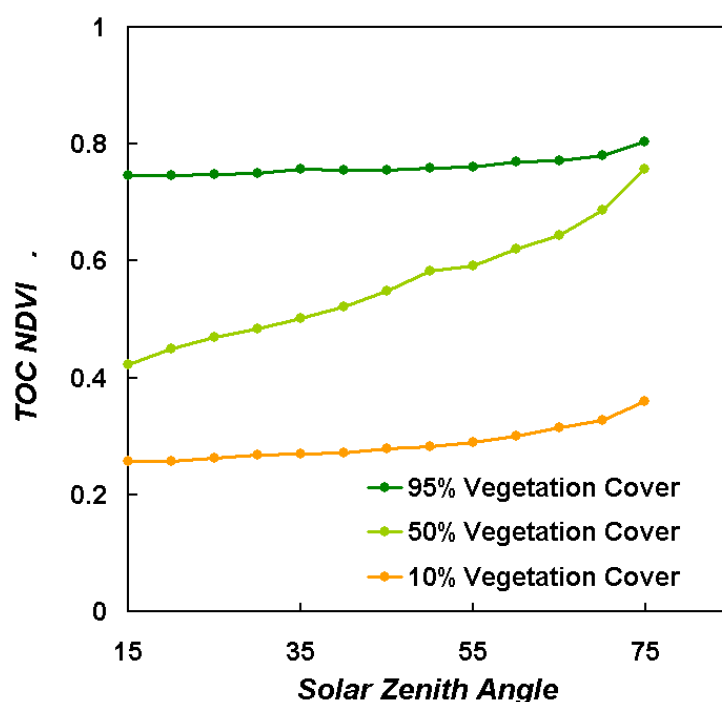
Fig. 3-2: *The effects of forest vegetation cover on the relationship between solar zenith angle (SZA) and top of the canopy (TOC) NDVI*

47

The combined impact of surface and atmospheric BRDF on AVHRR-NDVI time series is presented in Fig. 3-3 and Table 3-2. At the equator, the modeled TOC NDVI data for the site with 50% vegetation cover (Site-1) showed a positive trend of 0.0218 NDVI per year (Fig. 3-3 and Table 3-2), a trend that was greatly weakened at TOA to a mere 0.0061 NDVI per year. This was because, unlike surface BRDF, atmospheric components introduce a negative trend in NDVI with increase in SZA. The same phenomenon was also observed in NDVI time series data at the sites with 10%, and 95% vegetation cover, where a weak positive trend was removed. (Fig. 3-3; Table 3-2).

Latitude	Percent Tree Cover	Yearly Rate of change in NDVI	
		TOC	TOA
0	95	0.0033	-0.0053
0	50	0.0218	0.0061
0	10	0.0053	0.0000
30	95	0.0014	-0.0031
30	50	0.0148	0.0005
30	10	0.0049	-0.0004
60	95	0.0022	-0.0022
60	50	0.005	-0.0043
60	10	0.0038	-0.0017

Table 3-2: *Yearly rate of change in modeled AVHRR NDVI data for 5 years of NOAA-14 (Fig. 3-3). These trends were calculated by fitting linear regression lines to yearly average NDVI.*
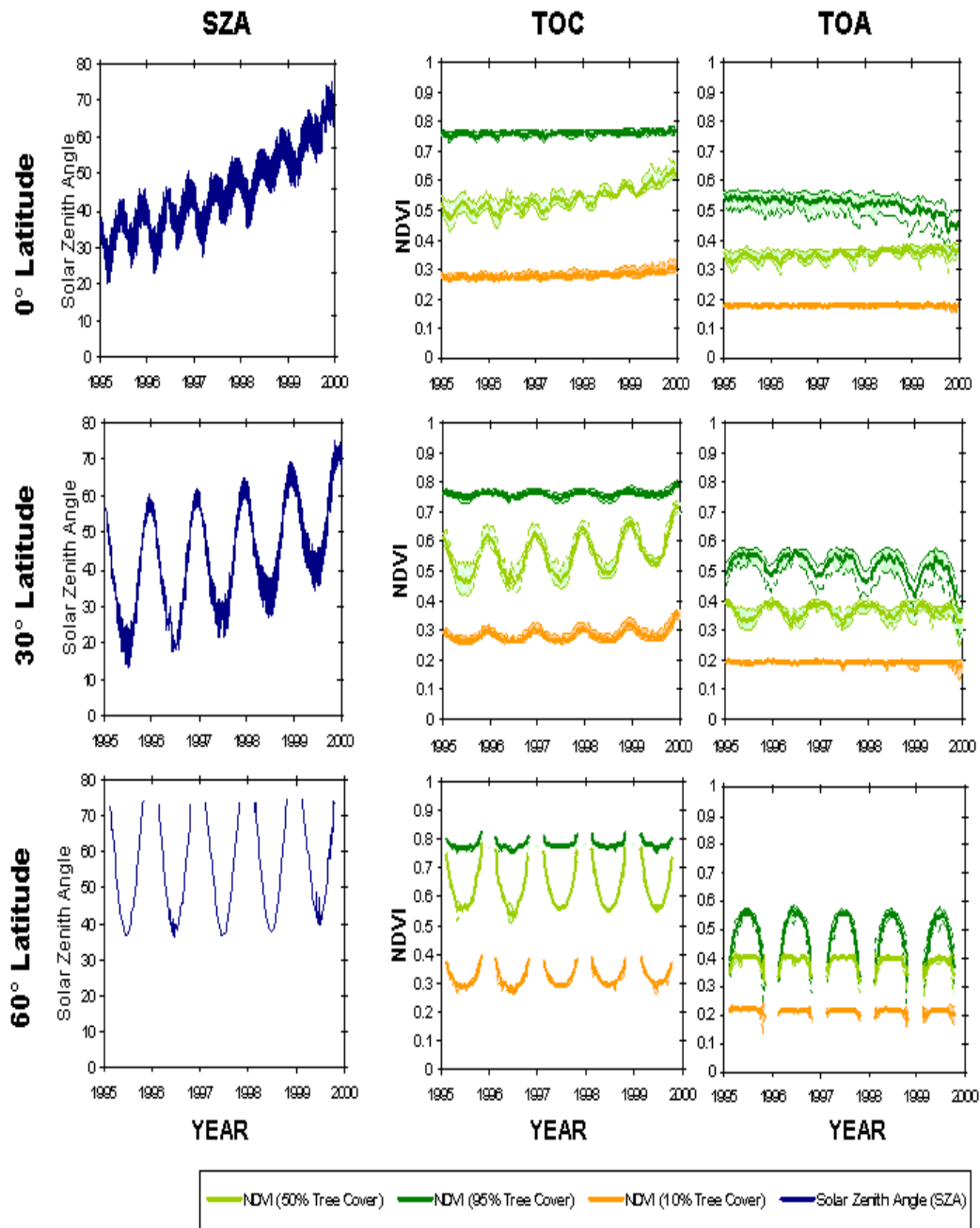
Fig. 3-3: *Impact of orbital drift on AVHRR data modeled for TOA and TOC NDVI data for first 5 years of NOAA-14 satellite's operational life (1995 to 1999) with various degrees of vegetation cover at 0°, 30°, and 60° latitudes. These time series were produced using FLIGHT canopy radiative transfer model and 6S atmospheric radiative transfer program. The simulation assumes evergreen vegetation cover and AOT = 0.15. **Note:** The high frequency variation observed in SZA, which is due to inclusion of data from multiple orbits, causes a similar high frequency variation in NDVI time series. The thick line represents a 10 day mean NDVI and the thinner lines (not always separable from the mean) represent the maximum and minimum value of NDVI for the same 10 day period.*

At 30° latitude the SZA had a weaker inter-annual trend leading to similarly weak inter annual trends in TOC NDVI. For example, at the site with 50% vegetation cover, the trend was only 0.0148 NDVI per year when compared to 0.0218 NDVI per year at equator. However there was a seasonal component to SZA which created intra-annual patterns similar to seasonal vegetation dynamics. At 50% vegetation cover, this seasonality was fairly prominent even in TOA NDVI data (Fig. 3-3; Table 3-2).

At 60° latitude there were practically no inter-annual trends in SZA, hence there were no inter-annual trends in either TOC or TOA NDVI. However there was a strong seasonal component to the SZA trend, which led to a similarly prominent, but false impression of seasonal vegetation dynamics in TOC NDVI data. Especially at beginning and end of the growing season, when SZA was very high, both the surface BRDF and the atmospheric impact were extreme and sometimes canceled each other out. This phenomenon could be seen in the TOA NDVI time series where both sites (50% and 10% vegetation cover) at 60° latitude showed no intra-annual variations, although there were strong intra-annual variations in TOC NDVI.

3.3.2. Effectiveness of MODIS BRDF parameters for BRDF correction of AVHRR NDVI time series data

Fig.3-4 demonstrates the effectiveness of MODIS BRDF parameters for normalization of the modeled AVHRR TOC NDVI to 45° SZA and 0° VZAs. The inter-annual trend of 0.02 NDVI units per year in TOC NDVI was reduced

50

considerably to a trend of 0.005 NDVI units per year for site 1 (~50% vegetation cover). The spurious seasonality was also considerably reduced. The TOC NDVI time series data for site 2 (~95% forest cover) had a weak inter-annual trend of 0.004 NDVI units per year which was only slightly affected by BRDF correction. However, the large inter-annual variation in near infrared was greatly reduced. The BRDF correction technique was further tested directly on AVHRR data from LTDR dataset (Fig. 3-5). Although the AVHRR data used for this study did not include correction for aerosol, the BRDF normalization improved surface reflectance and NDVI trends considerably. In both modeled TOC and actual AVHRR data the high frequency noise in red and NIR channels due to VZA variation was also effectively removed (Fig. 3-5).
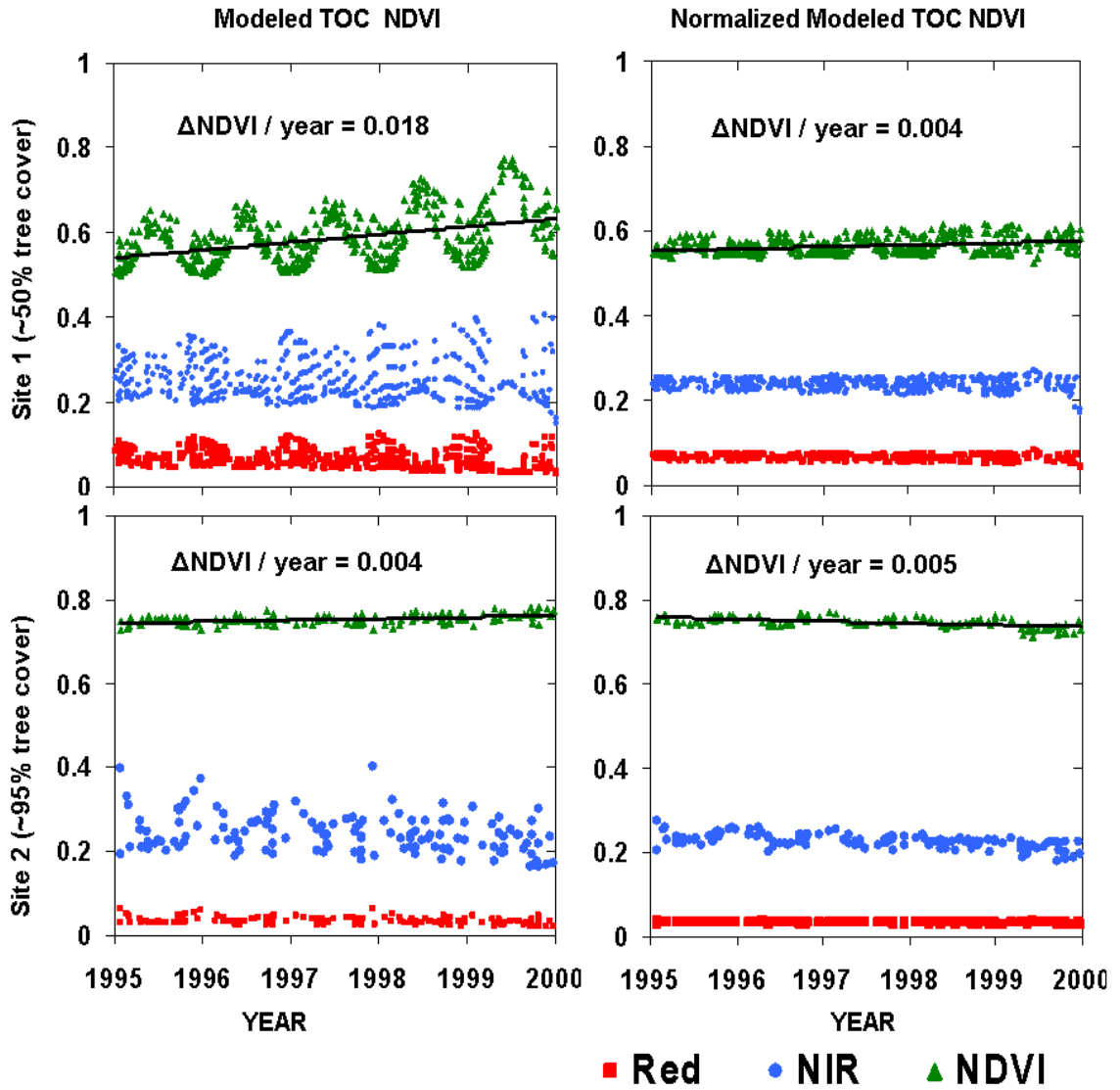
Fig. 3-4: *The effect of MODIS BRDF correction technique in removing the impact of orbital drift on top of canopy (TOC) NDVI data. On the left are the data without the BRDF correction and on the right are the data with the MODIS BRDF correction. Red, near infrared and NDVI are shown for 5 years of AVHRR data. The inter-annual NDVI trend was estimated by fitting a linear polynomial to yearly NDVI averages.*
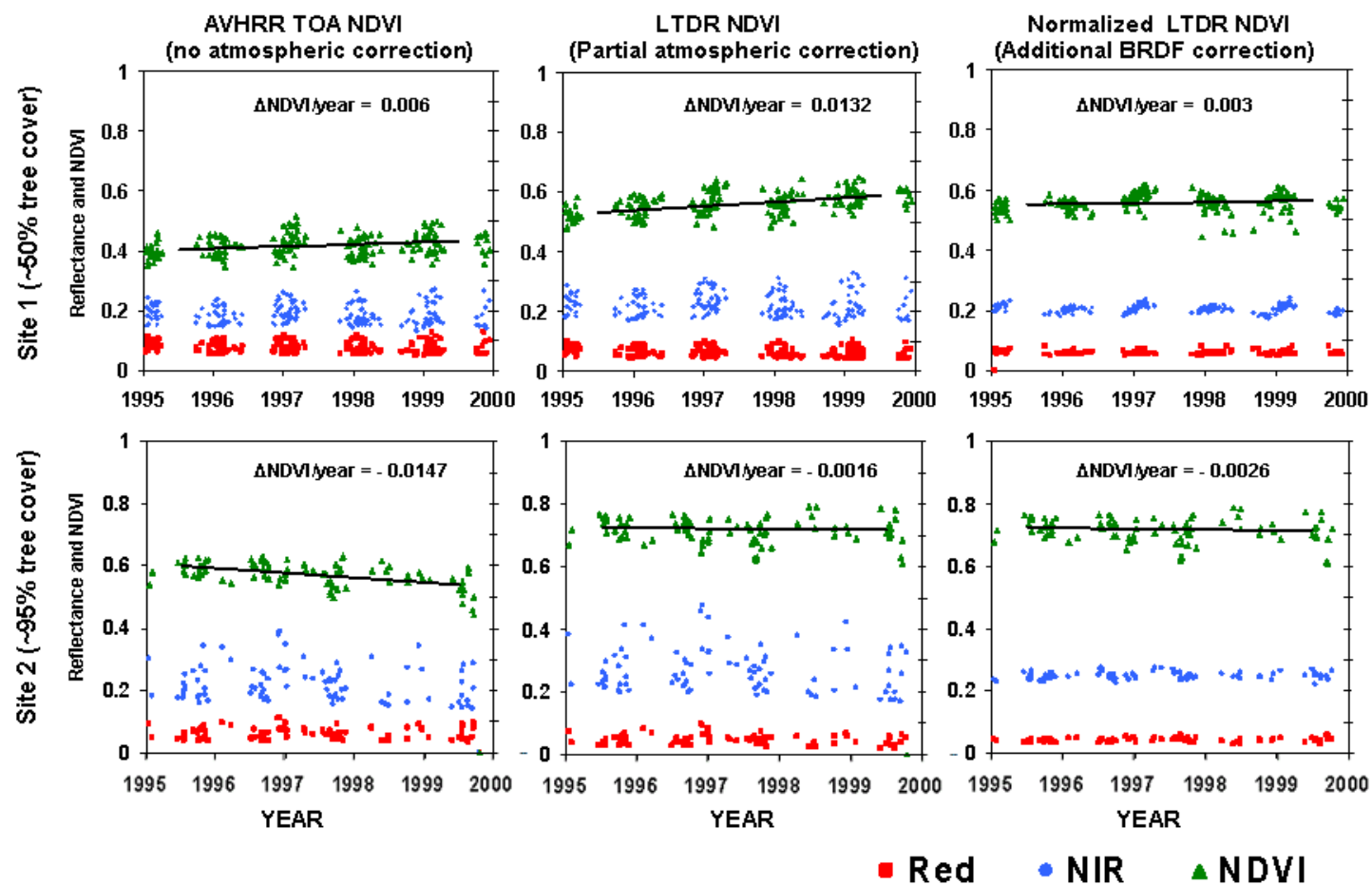
Fig. 3-5: *This figure shows the impact of different levels of correction on AVHRR NDVI time series data. It can be observed that atmospheric correction of LTDR NDVI data removes negative trends introduced by atmosphere and exposes positive trends due to surface BRDF. It also shows the effectiveness of MODIS BRDF correction technique in removing the positive trends introduced by surface BRDF. The inter-annual NDVI trend was estimated by fitting a linear polynomial to yearly NDVI averages.*

3.4. Conclusions

The analysis presented in this chapter indicates that the extent of vegetation cover is a crucial factor affecting sensitivity of TOC NDVI time series data to orbital drift. This sensitivity was found to be highest at vegetation cover close to 50%. At both 10% and 95% vegetation cover, the impact of SZA change on TOC NDVI was negligible (Fig. 3-2, 3-3). For dense tropical forest sites, the atmosphere was found to be the dominant source of inter-annual NDVI trends. SZA for sites at high latitudes showed prominent seasonality with very high solar zenith angles at the beginning and end of the growing season. At these high SZAs, impact of both surface and atmospheric BRDF was also extreme, thus severely decreasing the reliability of phenological metrics derived from NDVI data.

As noted before, TOC NDVI usually shows a positive relationship with solar zenith angle, while the atmosphere imposes a negative relationship in TOA NDVI data. It was observed that depending on the SZA, atmospheric composition, and vegetation cover of the site being studied, either one of these opposite relationships can dominate the other, sometimes even canceling each other out and causing a spurious improvement in the quality of the data. Thus the atmospheric correction exposed the surface BRDF effect on NDVI time series suppressed by atmospheric interference. Clearly with improvements in atmospheric correction, an operational BRDF correction technique significantly improves the precision of the AVHRR NDVI data. In this study it was found that the BRDF correction technique developed for MODIS data (Vermote et al. 2009a) provides a promising method to remove the

contribution of surface BRDF to the impact of orbital drift on NDVI and is worth applying to future developments of AVHRR processing such as the new LTDR archive.

Chapter 4: Quantification of Overall Uncertainty and Impact of Spatial and Temporal Aggregation

4.1. Introduction

Although previous investigations of uncertainty in the AVHRR NDVI data have given some valuable insights (Cihlar et al. 1998; Eklundh 1995; Fensholt et al. 2006a; Fensholt et al. 2006b; Gallo et al. 2005; Goward et al. 1993; Nagol et al. 2009), most of them, including the research presented in chapters 2 and 3, do not include all sources of uncertainty. AVHRR NDVI data are normally used with some kind of temporal as well as spatial aggregation (averaging, maximum value or median value compositing, etc) to reduce the impact of various shortcomings in the data processing. These compositing methods are generally believed to decrease uncertainty in the data considerably (Cihlar et al. 1994; Holben 1986), yet there have been no studies to quantify the extent of these positive effects. Bearing in mind the many influential studies of Earth system science that have been based on AVHRR NDVI, a better understanding of uncertainty is of critical importance. The purpose of the research presented in this chapter was to estimate uncertainty in AVHRR NDVI data and to investigate the impact of various degrees of spatial and temporal aggregation.

4.2. Data and methods

The uncertainty in AVHRR NDVI data was estimated by comparison with coincident data from MODIS Aqua instrument. The relatively low uncertainty in MODIS data (0.007 to 0.017 NDVI units) (Vermote et al. 2006) when compared to that of AVHRR data (0.0206 to 0.078 NDVI units) (chapter-2) makes this approach of estimating uncertainty reasonable. However, this method does not account for residual errors in the MODIS data itself, which can lead to an underestimation of uncertainty. The extent of this underestimation is indeterminable, because the spatial variability and the impact of spatial and temporal aggregation on the uncertainty in MODIS data is not yet determined. One chief advantage of using this framework is that, it allows the calculation of location specific estimates of uncertainty and also account for impacts of spatial and temporal aggregation.

The temporal overlap between NOAA-16 and MODIS Aqua instruments (2003-2006) was used for estimation of uncertainty. This study used NDVI data from three regions, Australia, the Sahel region in Africa, and Northern South-America, to sample a wide range of vegetation types and atmospheric compositions (Fig. 4-1).

The statistical framework defined in section 1.2.8 (chapter 1) was used to estimate uncertainty (random error) in the AVHRR NDVI data. The uncertainty statistic was calculated as the standard deviation of the data points relative to the systematic bias line. The systematic component (bias) was estimated by fitting a first order polynomial to the two dimensional scatter plot comparing AVHRR NDVI data to the reference data (MODIS Aqua data).
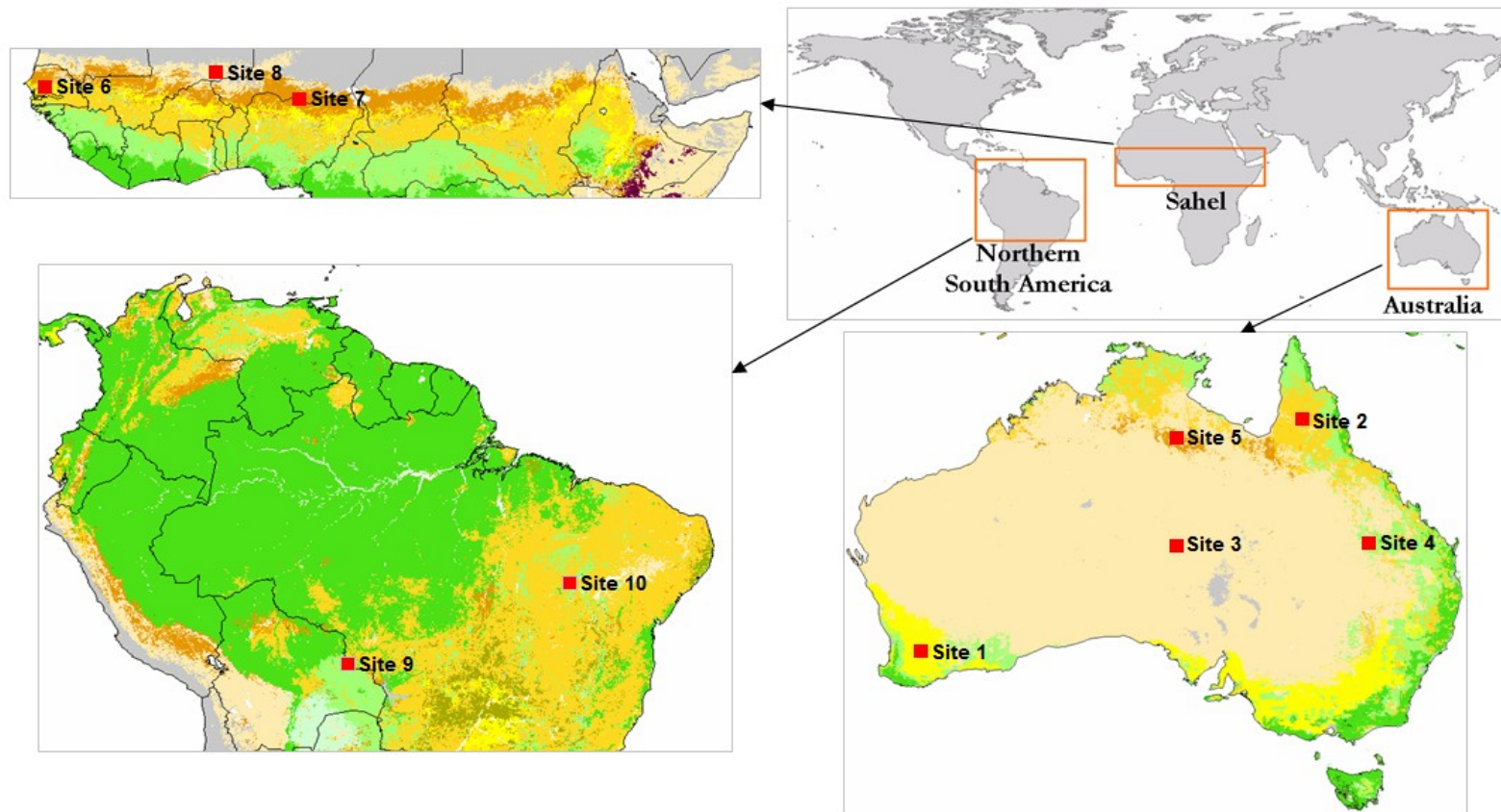
Australia

Fig. 4-1: *The three regions (Australia, Sahel, and northern South-America) and the locations of the sites (Table 4-1) where further study of the impact of spatial and temporal aggregation on uncertainty in AVHRR NDVI data was conducted.*

Site ID	Region	Land cover Type	long	lat
1	Australia	Cropland	117.80	-32.65
2	Australia	Savanna	143.00	-16.50
3	Australia	Open Shrubland	134.65	-25.30
4	Australia	Woody Savanna	147.75	-25.10
5	Australia	Mixed (Grassland / open Shrubland)	134.20	-17.55
6	Sahel (Africa)	Cropland	-15.65	14.15
7	Sahel (Africa)	Grassland	8.35	13.45
8	Sahel (Africa)	Open Shrubland	-0.45	15.90
9	Northern South America	Mixed (Forest / Bare)	-45.40	-10.10
10	Northern South America	Mixed (Woody Savanna / Cropland)	-59.95	-16.00

Table 4-1: *Locations and land cover of the sites in Australia, Sahel region of Africa, and Northern South America where further study of impact of spatiotemporal aggregation on AVHRR NDVI uncertainty and its implication for study of inter-annual NDVI time series trends was carried out.*

4.2.1. AVHRR data

The AVHRR NDVI data from LTDR version-3 dataset were used in this study (http://ltdr.nascom. nasa.gov/ltdr/ltdr.html) (Pedelty et al. 2007). The product includes daily NDVI as well as surface reflectance data at a spatial resolution of 0.05°, which matches the Climate Modeling Grid (CMG) used for MODIS Terra and Aqua.

The LTDR preprocessing includes vicarious calibration, atmospheric correction for Rayleigh scattering, ozone, and water vapor, and an improved cloud mask technique (Vermote et al. 2009b). The AVHRR data were normalized to a uniform sun-sensor geometry using the BRDF correction technique developed for MODIS data (Vermote et al. 2009a). This technique has been demonstrated to be

reasonably effective in removing the impact of orbital drift on AVHRR NDVI data (chapter 3).

4.2.2. Reference data (MODIS Aqua data)

The MODIS Aqua based CMG surface reflectance product (MYD09CMG) was used as reference data for estimating the uncertainty in LTDR AVHRR NDVI data. Data from MODIS Terra instrument were not included because of a more than 4 hours of difference in overpass time when compared to AVHRR instruments, while Aqua platform has a near simultaneous overpass.

The MODIS CMG data product is estimated daily on a 0.05 degree grid using MODIS Level-1B bands 1-7 (459-2155nm). The MODIS CMG atmospheric correction scheme accounts for the effects of atmospheric gases, aerosols, and thin cirrus clouds. The data were further corrected for BRDF effect using the technique proposed by Vermote et al., (2009).

4.2.3. Impact of Spatial and Temporal Aggregation on AVHRR NDVI Uncertainty (Random Error)

The impact of spatial aggregation on the uncertainty in AVHRR NDVI data was investigated by comparison with reference data at various levels of spatial aggregation (1x1, 3x3, 5x5, 7x7 pixel matrix averages) for the dominant land cover types in the three regions (Australia, Sahel, and northern South-America) (Fig. 4-1). Since NDVI is a non-linear transformation, the spatial aggregation was performed in

the spectral domain before calculation of NDVI. A land cover map derived from MODIS data (MOD12C1) for year 2004 was used in the analysis. MOD12C1 has a resolution of 0.05 degrees and is derived with the same algorithm used in the Global 1 km Land Cover Type product (MOD12Q1) (Hodges 2002). This product contains three classification schemes, of which, IGBP (International Geosphere Biosphere Programme) global vegetation classification scheme was used in this study. The map gives the dominant land cover type and the sub-grid frequency of the other land cover classes.

All the pixels in each dominant land cover type, except the ones on the edge of the land cover patches, were included in the calculation of final precision statistic for that land cover type. Any spatially aggregated pixels with even one cloud contaminated pixel were excluded. Impact of commonly used temporal compositing techniques were investigated only for 3x3pixel spatial aggregates. The temporal compositing techniques included in this analysis were: 1) monthly maximum value, 2) monthly median, 3) monthly average, 4) quarterly average, and 5) yearly average.

4.2.4. Estimation of Location Specific Uncertainty and Evaluation of the Significance of Interannual Trends

In previous sections overall uncertainty estimates for different land cover types in various regions were addressed. However uncertainty at different locations within a land cover type can show significant variations, the impact of sub-pixel variability in NDVI was also not accounted for. AVHRR NDVI data from the same dataset, depending on the spatial and temporal compositing scheme used, can have

different degrees uncertainty. This makes it necessary for an AVHRR NDVI data user to estimate uncertainty for the specific location and aggregation scheme they have chosen to use.

Here ten sites from Australia, northern South America, and Sahel region of Africa (Table 4-1; Fig. 4-1) were used to illustrate the method for estimation of uncertainy in AVHRR NDVI data for specific locations and aggregation schemes. Two aggregation schemes involving spatial aggregation over 0.15ºx0.15º area (3x3 pixels) and 0.45ºx0.45º area (9x9 pixels) and temporal aggregation over a month were examined.

Using the uncertainty estimates for AVHRR NDVI data, to evaluate the significance of the observed inter-annual trends involves a few additional steps. Of the two aggregation schemes examined the one involving spatial aggregation over 9x9pixel area was used to illustrate these steps. The 18 year period (1982 to 1999) was used for the trend analyses. To use the uncertainty estimates for validation of observed inter-annual NDVI change in pre NOAA-16 era (year ≤2000), it was necessary to assume that the LTDR V3 processing sufficiently deals with the systematic errors arising from sensor degradation, and orbital drift.

The inter-annual trends in AVHRR NDVI data were calculated using the method utilized by Donohue et al., (2009) for calculating inter-annual fPAR trends in Australia. This method uses linear (ordinary least squares) regressions on a month-by-month basis. Trends were estimated for each of the twelve months in the year (e.g., trend for January, February, March, etc.). Because these regressions are linear, the yearly or seasonal inter-annual trends can be estimated by averaging the monthly

trends. The inter-annual trend calculated using this method is less vulnerable to data gaps.

The uncertainty estimate for each monthly inter-annual trend was calculated by introducing the NDVI uncertainty into the linear regression model as measurement error. The uncertainty in inter-annual trend estimated in this manner is a combination of measurement error (uncertainty in AVHRR NDVI data) and coefficient of determination (R-squared) of the linear regression model. Due to this the uncertainty estimates are sensitive to the length of time series and the data gaps also. The uncertainty statistic for the yearly inter-annual NDVI trend was then estimated by calculating quadratic mean of the uncertainty in the twelve monthly trends. The goal here was to demonstrate the calculation of thresholds for inter-annual NDVI change that must be exceeded for the observed trends to be considered significant.

4.3. Results

4.3.1. Impact of Spatial and Temporal Aggregation on AVHRR NDVI Uncertainty (Random Error)
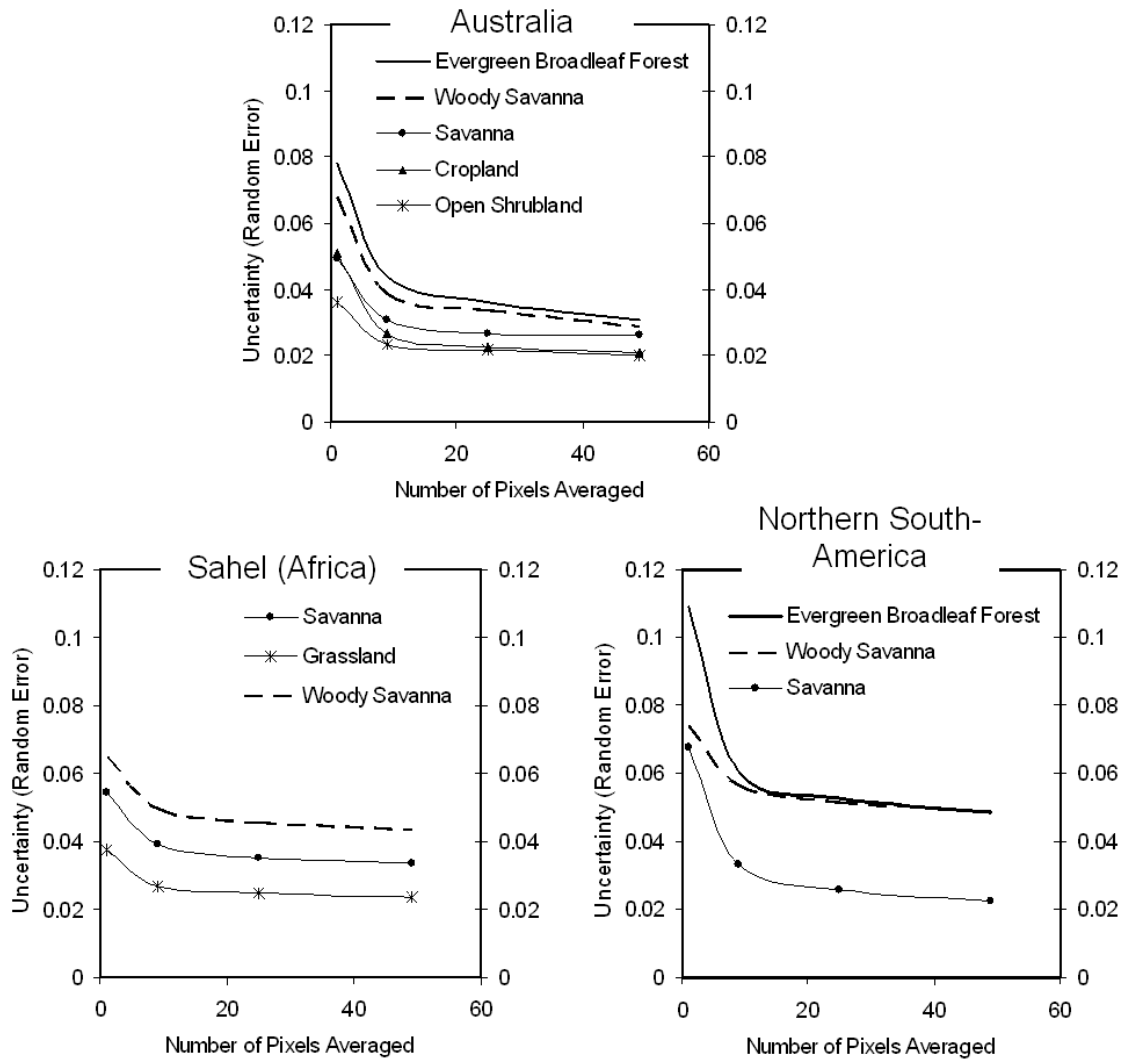
Fig. 4-2: *Impact of spatial aggregation on uncertainty in LTDR AVHRR NDVI data. The spatial aggregation was performed in the spectral domain before calculation of NDVI.*

Uncertainty in the LTDR AVHRR NDVI data, to which no spatial or temporal aggregation was applied, varied from 0.036 in Australian open shrub-land to 0.11 for evergreen broadleaf forests in northern South-America (Fig. 4-2). The investigation into the impact of spatial aggregation (Fig. 4-2) revealed that the uncertainty in AVHRR NDVI data decreases greatly as more pixels are aggregated. Even a 3x3pixel (9 pixels) aggregation considerably reduced the uncertainty in the data for all the land cover types in the three regions. For example, just by aggregation over 3x3 pixel matrices, the uncertainty in AVHRR NDVI measures in northern South-American evergreen broadleaf forests decreased from 0.11 to 0.06. Further aggregation over 7x7 pixel matrices (49 pixels) further decreased the uncertainty to 0.048 NDVI units. The uncertainty for Australian woody savanna showed a similar improvement from 0.068 to 0.039, and 0.029 at 3x3 and 7x7 pixel aggregation respectively. Uncertainty for other land cover types from all three regions, including Sahel, showed similar improvements. Most of the improvement was achieved with 3x3 pixel aggregation step. Although further spatial aggregation resulted in some reduction in uncertainty, it was relatively small (Fig. 4-2). Because of this, all further analyses of errors in AVHRR NDVI data were conducted on 3x3 pixel aggregates.

Investigation into the impact of three different monthly temporal aggregation schemes (maximum value, median, and average) conducted on 3x3pixel spatial aggregates (Fig.4-3) revealed that all three of these compositing schemes resulted in only slight decrease in uncertainty.
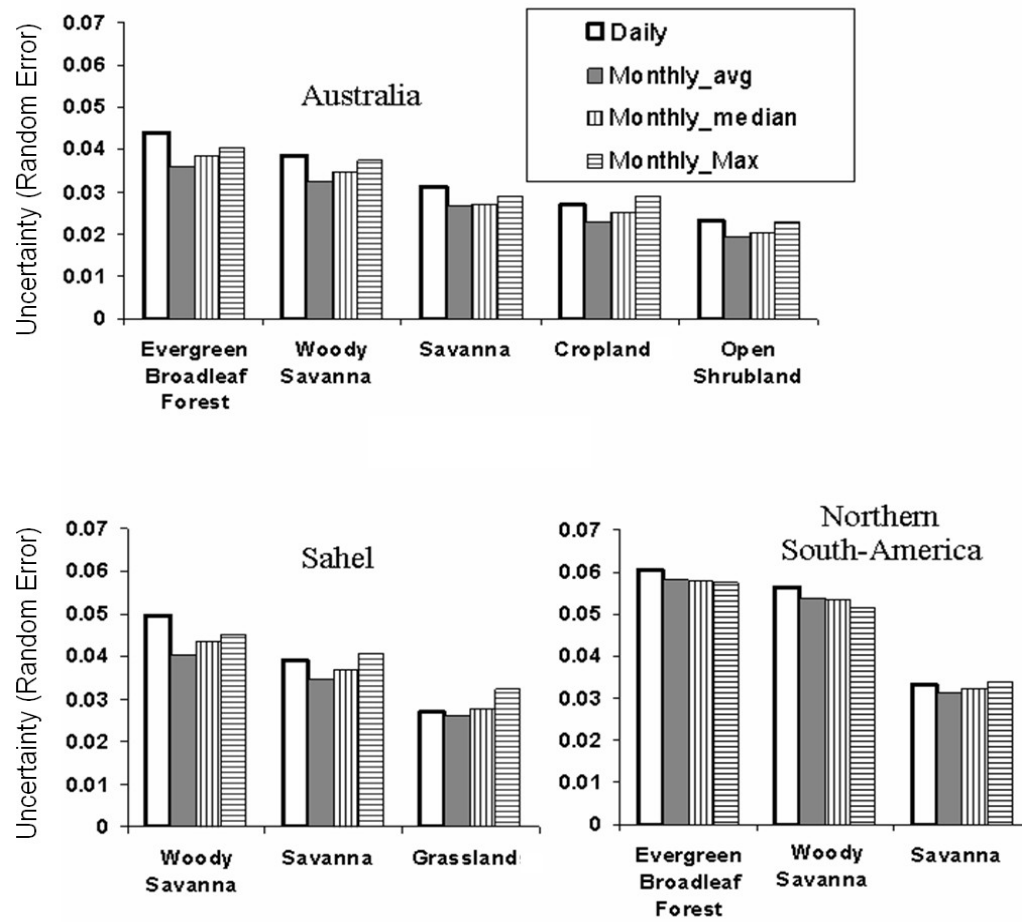
Fig. 4-3: *Impact of various types of monthly temporal compositing techniques on uncertainty in LTDR AVHRR NDVI data.*
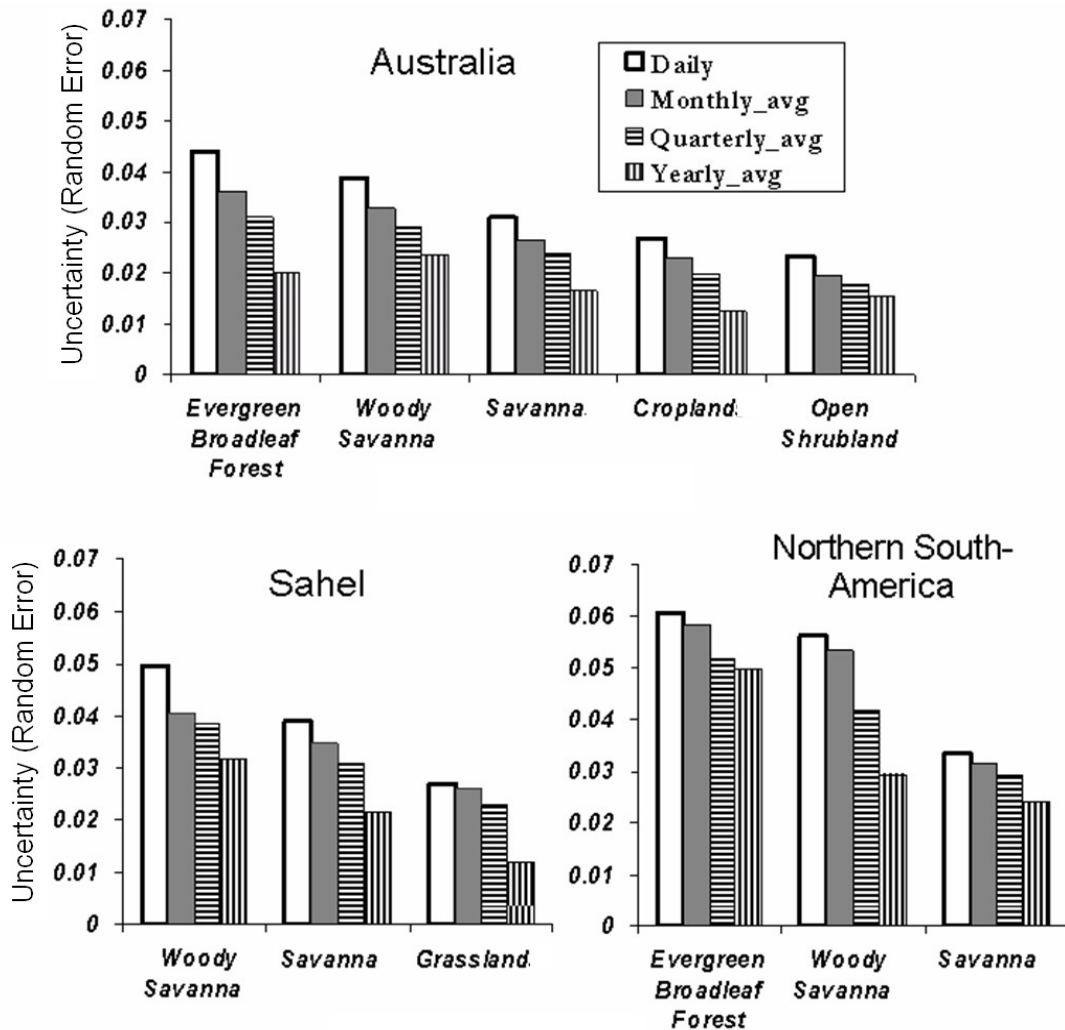
Fig. 4-4: *Impact of the temporal extent of aggregation on uncertainty in LTDR AVHRR NDVI data*

A consistent decrease in uncertainty was observed with increase in temporal extent of aggregation (Fig. 4-4). For example, the uncertainty in AVHRR NDVI in Australian evergreen broadleaf forests decreased from 0.044 NDVI units for daily data to 0.036, 0.031, and 0.020 NDVI units for monthly, quarterly, and yearly temporal aggregation respectively. The uncertainty for northern South-American woody savanna showed a similar reduction of uncertainty from 0.056 NDVI units for

daily data to 0.054, 0.042, and 0.029 NDVI units for monthly, quarterly, and yearly temporal aggregation respectively. Most of the other land cover types in all three regions showed similar pattern. However for northern South-American evergreen broadleaf forests, even yearly aggregation resulted in only ~10% (0.01 NDVI units) reductions in uncertainty. This may be due consistently hazy atmospheric conditions and limited availability of cloud free days.
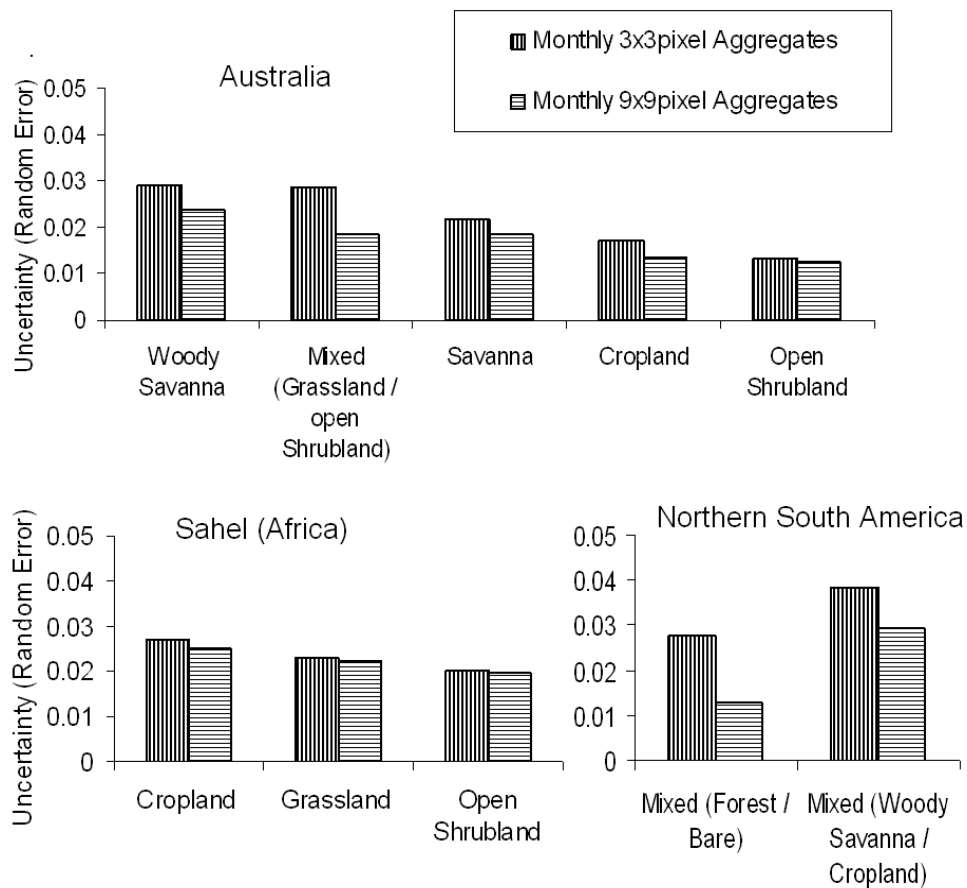
Fig. 4-5: *The LTDR AVHRR NDVI uncertainty at the 10 study sites (Table 4-1).*

The examination of the location specific uncertainty estimates for monthly 3x3 and 9x9 pixel aggregates for the 10 sites (Fig. 4-5) revealed that sites with sub-pixel heterogeneity in NDVI benefited more by spatial aggregation. For example the uncertainty in AVHRR NDVI data for the mixed (grassland/open shrubland) site in Australia decreased from 0.028 to 0.018 NDVI units and the uncertainty for the mixed (Forest / Bare) site in northern South America decreased from 0.028 to 0.012 NDVI units (Fig. 4-5). Similar improvements were observed at mixed (woody savanna / cropland) site in northern South America and the woody savanna site in Australia. On the other hand, increase in spatial extent of aggregation from 3x3pixel area to 9x9 pixel area had little impact on uncertainty estimates at sites which were homogeneous, e.g. the cropland, grassland, and open shrubland sites in Sahel and the open sbrubland site in Australia ,

The validation of the inter-annual NDVI change for 18 years (1982 to 1999) at the 10 sites (Fig. 4-6) revealed that only two sites, the grassland site (0.027 NDVI/18years) and the open shrubland site (0.028 NDVI/18years) in the Sahel, showed an NDVI change significant at 67% confidence interval. Only the cropland site in Australia showed an NDVI change (0.07 NDVI/18years) that was significant at 95% confidence interval. Although the Australian savanna site showed an NDVI change of 0.047 NDVI/18 years, it was not significant at even 67% confidence interval (Fig. 4-6). This showed that higher NDVI change does not always result in higher confidence.
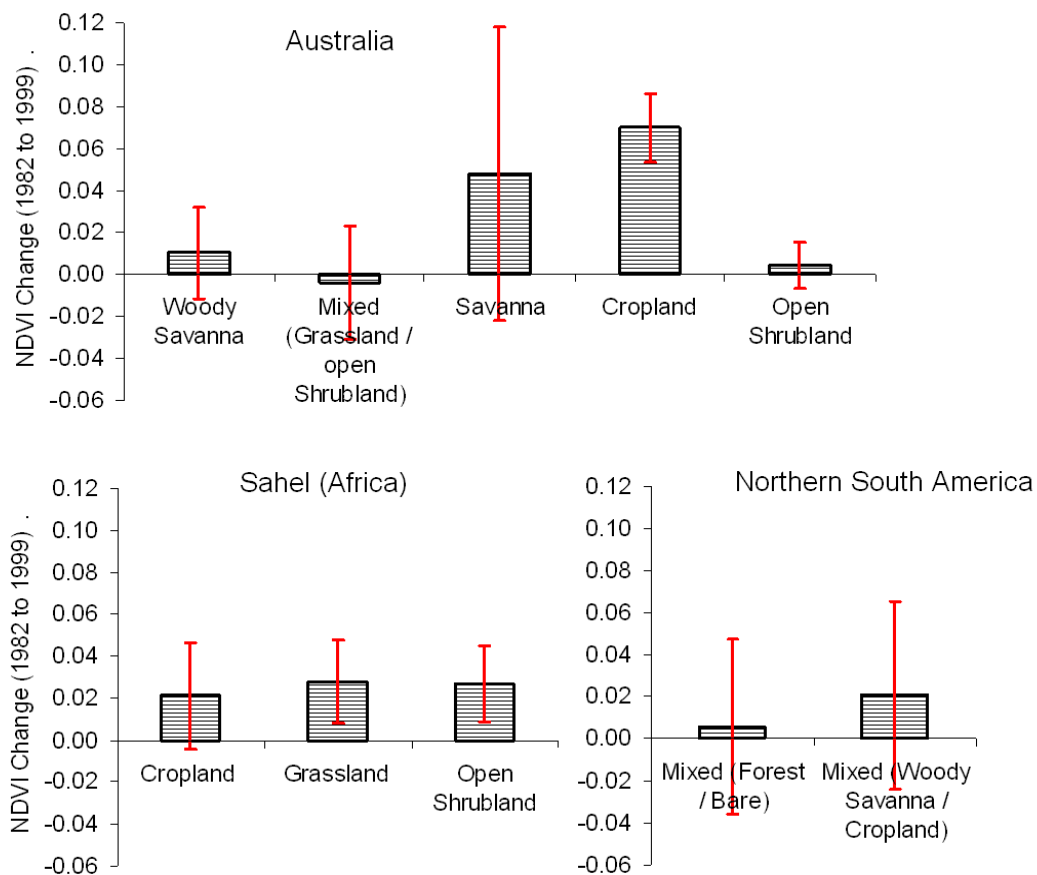
Fig. 4-6: *Total NDVI change observed in the 18 year time period of 1982 to 1999. The red lines represent the uncertainty.*

4.4. Discussion

The uncertainty estimates for un-aggregated LTDR AVHRR NDVI (0.036 to 0.11 NDVI units) (Fig. 4-2) were found to be much higher than the inter-annual change considered significant by many previous studies (Jia et al. 2003; Piao et al. 2003; Piao et al. 2006; Slayback et al. 2003; Young and Harris 2005). Most of this uncertainty can be ascribed to lack of comprehensive atmospheric correction in AVHRR dataset (Pedelty et al. 2007). Because the GAC sampling scheme can select a different sub-pixel area on every overpass, high sub-pixel variability in NDVI can considerably increase the uncertainty.

It was observed that even limited spatial aggregation of 3x3 pixels (0.15x0.15 degrees) reduced the uncertainty considerably. However, sites with high sub-pixel heterogeneity benefited from further spatial aggregation (Fig. 4-5). The results presented in section 4.3.1 (Fig.4-2) showed that degrading the resolution of AVHRR data from 0.05 degrees to 0.15 degrees is a reasonable technique for reduction of uncertainty in AVHRR NDVI data. For many applications the benefit due to the reduction of uncertainty achieved in this way would outweigh the disadvantages due to decrease in spatial resolution.

It was also observed that, after 3x3pixel spatial aggregation, temporal aggregation to monthly time period resulted in only slight reduction in uncertainty (Fig. 4-3). The temporal aggregation of data to which no spatial aggregation was applied was also found to reduce uncertainty, but to a limited extent only. Moreover, in many parts of the world the temporal aggregation method is severely limited by the number of cloud free days available during a compositing period

Of the three monthly temporal compositing techniques tested (maximum value, median, and average), the monthly averaging technique produced slightly but consistently better results. This is in contrast with the general understanding that MVC is the best compositing technique. This can be attributed to better cloud masks, improved atmospheric correction, and BRDF correction employed in the LTDR dataset when compared to earlier AVHRR NDVI datasets. These improvements in the data processing make the ability of MVC technique to decrease the impact of partial atmospheric correction and inaccurate cloud masks redundant.

The technique of evaluation of AVHRR NDVI data by comparison with MODIS data allows for estimation of uncertainty at any geographic location and aggregation scheme (Fig.4-5). This location-specific uncertainty can then be used to evaluate the significance of observed inter-annual NDVI trends and anomalies (Fig. 4.6). This technique accounts for spatial heterogeneity of uncertainty in the AVHRR NDVI data as well as the impact of the specific spatial and temporal aggregation scheme being used. However, to be able to use the uncertainty estimates derived using data from years 2003 to 2006 to evaluate the observed inter-annual NDVI trends and anomalies in pre 2000 era, it is necessary to make sure that there is no significant sensor degradation, and orbital drift related non-stationarity in the data.

4.5. Conclusions

This study empirically demonstrated that, in many regions, minimal spatiotemporal aggregation considerably decreases the uncertainty in the LTDR AVHRR NDVI data. Aggregation beyond 3x3 pixels was found useful at sites with high sub-pixel NDVI heterogeneity.

The framework for estimation of uncertainty presented in this chapter not only accounts for the impact of spatial and temporal aggregation but also provides a way to calculate location specific error estimates. These error estimates can be used to set informed confidence intervals for future global change and regional studies of inter-annual vegetation dynamics.

Chapter 5: Overview and Discussion

The goal of this dissertation was to systematically investigate and quantify the uncertainty in AVHRR NDVI data. The primary sources of uncertainty in the NDVI datasets derived from NOAA AVHRR data are: 1) partial atmospheric correction; 2) orbital drift; 3) sensor degradation; and 4) geolocation error. The second chapter of this dissertation investigated the impact of partial atmospheric correction and the third chapter dealt with non-stationarity introduced by orbital drift in the AVHRR NDVI time-series data. In the fourth chapter, instead of quantifying uncertainty from individual sources and then accounting for the complex interactions between each of them, overall uncertainty in AVHRR NDVI data was estimated directly by comparison with MODIS data for the years 2002-2006, the overlap period between the two sensors (MODIS Aqua and NOAA-16 AVHRR). This technique also facilitated the investigation of the impact of spatial and temporal aggregation. Next section will give an overview of the results from second, third, and fourth chapters followed by a discussion of implications of these results

5.1. Overview of the Results

The incompleteness or absence of atmospheric correction is a major source of uncertainty in the AVHRR NDVI data. The research presented in chapter 2 assessed the uncertainty due to this shortcoming in three publicly available, processed AVHRR NDVI datasets (LTDR, PAL, and TOA). This assessment revealed that, of the three AVHRR NDVI datasets investigated, LTDR dataset has the lowest uncertainty. Uncertainty estimates for the LTDR dataset were found to be 0.021, 0.037, and 0.078

NDVI units for clear, average, and hazy atmospheric conditions respectively (Fig. 5-1; Table 2-1).
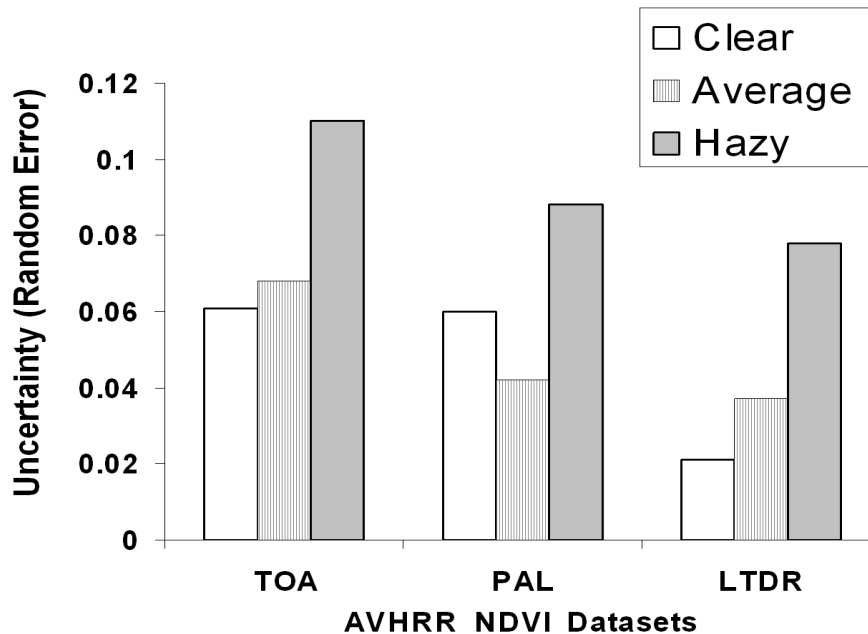
Fig. 5-1: *Summary of results from Chapter 2. Uncertainty in NDVI for TOA, PAL, and LTDR datasets (Table 2-1).*

AVHRR NDVI data is nearly always used with some form of temporal compositing to decrease the impact of atmospheric interference and residual cloud contamination. For example, the GIMMS dataset is available with 15 day maximum value compositing and PAL dataset is available with 10 day and monthly maximum value compositing. Even LTDR dataset, which provides daily NDVI data, has been used with temporal compositing (Alcaraz-Segura et al. 2010). In most cases AVHRR NDVI data are further spatially aggregated, sometimes over vast regions. The spatial and temporal aggregation is generally claimed to decrease the uncertainty

considerably (Cihlar et al. 1998; Cihlar et al. 1994; Holben 1986). However, due to limited spatial and temporal coverage of AERONET data, the analysis presented in chapter 2 could not account for these improvements. The spatial heterogeneity of uncertainty was also not addressed. One more limitation was that, the network of AERONET sites did not sample all land cover types and latitudinal zones (Fig. 2-2).

Another major shortcoming in the AVHRR NDVI data is the non-stationarity caused by orbital drift. The orbital drift related non-stationarity in AVHRR NDVI time-series, not only hinders the detection and interpretation of inter-annual vegetation dynamics; it also flouts the assumption of normal distribution essential for estimation of the uncertainty. The third chapter of this dissertation investigated the impact of this shortcoming and the effectiveness of BRDF correction technique proposed by Vermote et al., (2009) in dealing with it.

The results indicated that, for sites with dense as well as sparse vegetation cover, atmosphere is the primary source of the orbital-drift-related, inter-annual NDVI trends. However, at vegetation cover close to 50%, the surface BRDF effect was the dominant source. Investigation into effectiveness of the BRDF correction technique (Vermote et al. 2009) indicated it to be a promising method for reducing the contribution of surface BRDF to the impact of orbital drift. Some of the positive attributes of this method are: 1) It does not require an a priori knowledge of the land cover type and vegetation structure; and 2) limited availability of cloud free data, does not affect the derivation of BRDF parameters.

However the BRDF correction method does not address the spurious negative inter-annual NDVI trends caused by systematic increase in atmospheric path length due to

orbital drift. The term "spurious trend" here refers to the inter-annual trend in AVHRR NDVI time-series data caused, not by actual vegetation dynamics on earth surface, but by orbital drift or other shortcomings in the sensor system and post-processing. The magnitude of this trend can be estimated as the inter-annual trend of AVHRR and MODIS-Aqua NDVI differences (AVHRR NDVI – MODIS-Aqua data). Fig. 5-2 (site-2) illustrates the presence of the spurious negative trends using data at an agricultural site in eastern Henan province of China, as an example. More than 60% of the data at this site had AOT greater than 0.25. This constant hazy atmosphere and an annual 4° SZA increase due to orbital drift resulted in a spurious negative inter-annual trend of 0.02 NDVI units for the four year period (2003-2006). The spurious negative inter-annual trends in AVHRR NDVI data were also observed in other regions like Sub-Sahelian tropical savannas, tropical forests, and in regions where occurrence of high AOT coincided with peak growing season.

In some vegetated hilly regions spurious positive NDVI trends were also observed. Fig. 5-2 (site-1) illustrates this using a site in north eastern Himalayan region. At this site an annual SZA increase of 4° during the four year period of 2003 to 2006 resulted in a corresponding spurious positive inter-annual trend of 0.052 NDVI units. Similar prominent trends were also observed in other vegetated hilly regions near Himalayan, and Andes mountain ranges.
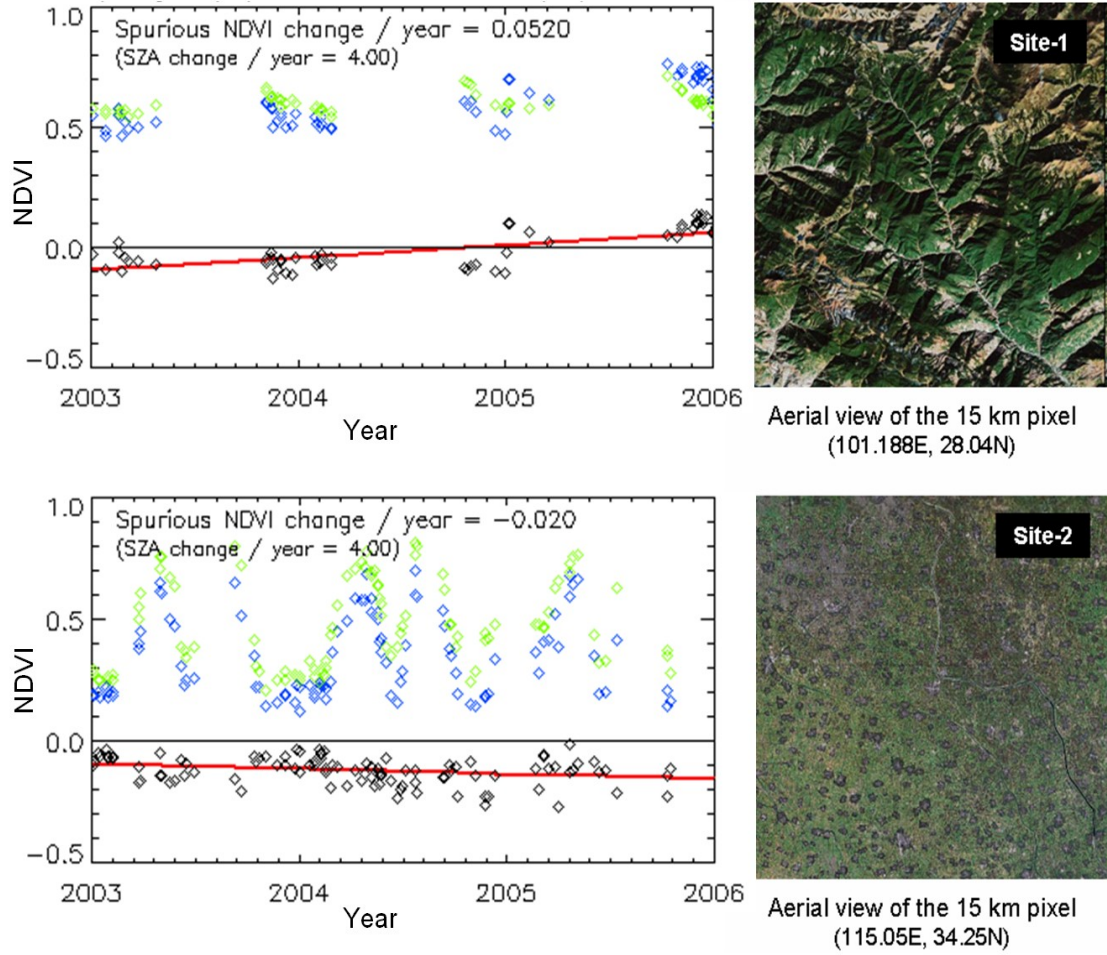
Fig. 5-2: *Examples of orbital drift related spurious inter-annual NDVI trends. The green, blue, and black colored data represent MODIS Aqua NDVI data, AVHRR NDVI data, and the difference between these two data (AVHRR NDVI - MODIS NDVI) respectively. The thick red line represents the spurious inter-annual trend. The magnitude of the spurious NDVI trend was determined by estimating slope of the linear curve fitted to the LTDR AVHRR NDVI and MODIS-Aqua data differences. Site-1 (115.05E, 34.25N) is located in vegetated hilly regions of northeastern Himalayan range. Site-2 (101.188E, 28.04N) has mixed agricultural and urban/built-up land cover and is located in Eastern Henan province of China.*

The results presented in the second and third chapters of this dissertation dealt with individual sources of uncertainty. The goal of the research presented in fourth chapter was to estimate the overall uncertainty in the AVHRR NDVI data directly by comparison with MODIS data. The impact of temporal and spatial aggregation was also examined.

Only LTDR AVHRR NDVI dataset was included in this analysis. GIMMS dataset was excluded because its processing includes temporal smoothing, removal of non-vegetation NDVI signal, and manipulation of dynamic range making the direct comparison of individual NDVI data to the MODIS data unreasonable. The lack of BRDF correction in GIMMS data further complicates the situation.

Investigation into the impact of various degrees of spatial aggregation (Fig. 4-4 to 4-7) on the uncertainty in LTDR AVHRR NDVI data (section 4.2.1) indicated that minimal spatial aggregation (3x3 pixel spatial averaging) decreased the uncertainty considerably. Further spatial aggregation was generally found to be of little benefit (Fig. 4-5).

5.2. Global Uncertainty Maps

The method of location specific uncertainty estimation discussed in chapter 4 can be used to create global and regional uncertainty maps for various spatial and temporal aggregation schemes. These maps can then be used to evaluate and understand the significance of inter-annual trends and anomalies in LTDR AVHRR NDVI data. Fig. 5-3 presents an example of an uncertainty map for LTDR AVHRR NDVI data with a 3x3 pixel spatial aggregation. This uncertainty map revealed a considerable amount of spatial heterogeneity of uncertainty.
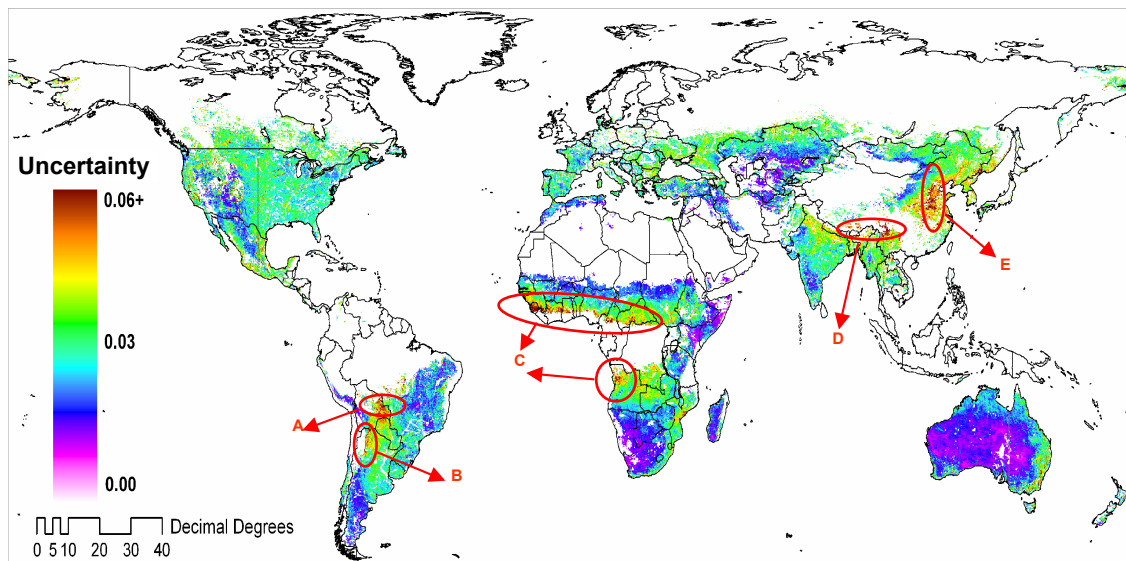
Fig. 5-3: *Global uncertainty map of 3x3 pixel spatial aggregates (averages) for LTDR AVHRR NDVI data. Deserts, urban areas, wetlands, and the pixels with less than 30 data points were excluded from the analysis.*
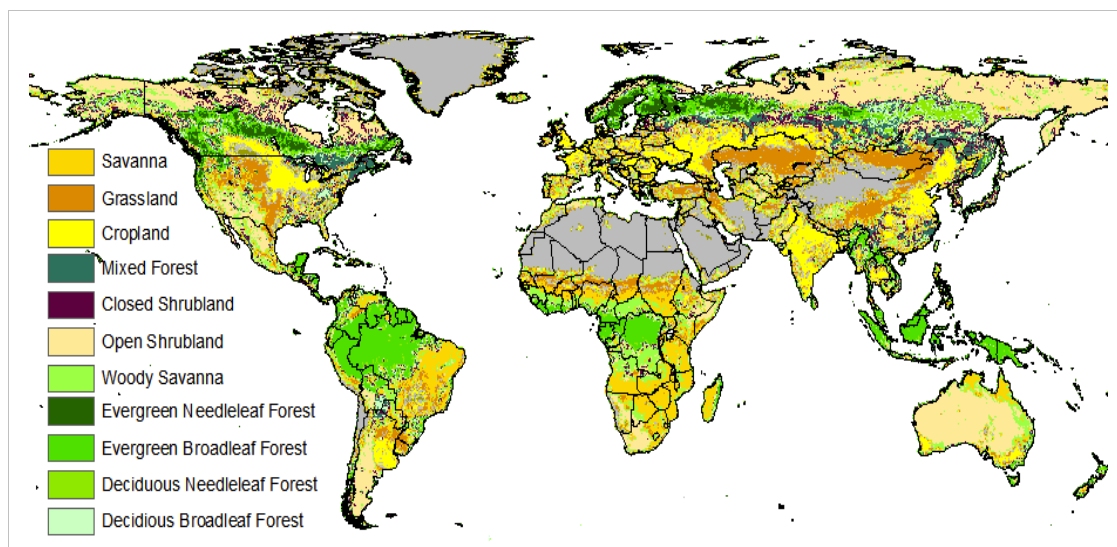
Fig. 5-4: *Land cover map derived from MODIS data (MOD12C1) for year 2004 with IGBP classification schemes*

The regions with low vegetation cover, like the open shrublands in Australia, southern Africa, southern South America, and southern North America showed uncertainty close to 0.02 NDVI units (Fig. 5-3; Fig. 5-4). Parts of grasslands in central Asia and Sahelian region also showed similarly low uncertainty (Fig. 5-3; Fig. 5-4). This can be attributed to low sensitivity of NDVI to atmospheric interference as well as BRDF effect, in sparsely vegetated regions (section 3.3.1; Fig. 3-2: Fig. 3-3).

Relatively high uncertainty was observed in regions with denser vegetation cover, like croplands, savannas, and forests. This may be due to higher sensitivity to atmospheric interference (Fig. 3-2). Uncertainty estimates higher than 0.035 were observed for many pixels in regions like the sub-Sahelian savannas, Bolivian tropical forests, and croplands in Indian Gangetic plains, North America, and eastern China, where high NDVI and high AOT occur simultaneously (Fig. 5-3; Fig. 5-4).

In some regions (Fig. 5-3: Regions A, C, E) the non-stationarity in the AVHRR NDVI time-series data, due to atmospheric BRDF and orbital drift (Fig. 5-2: Site-2), was a significant contributor to the high uncertainty (> 0.06 NDVI units). Similarly high uncertainty estimates were also observed in some vegetated hilly regions (Fig. 5-3: Regions B, D). This can be attributed to surface BRDF related non-stationarity described in Fig. 5-2 (Site-1).
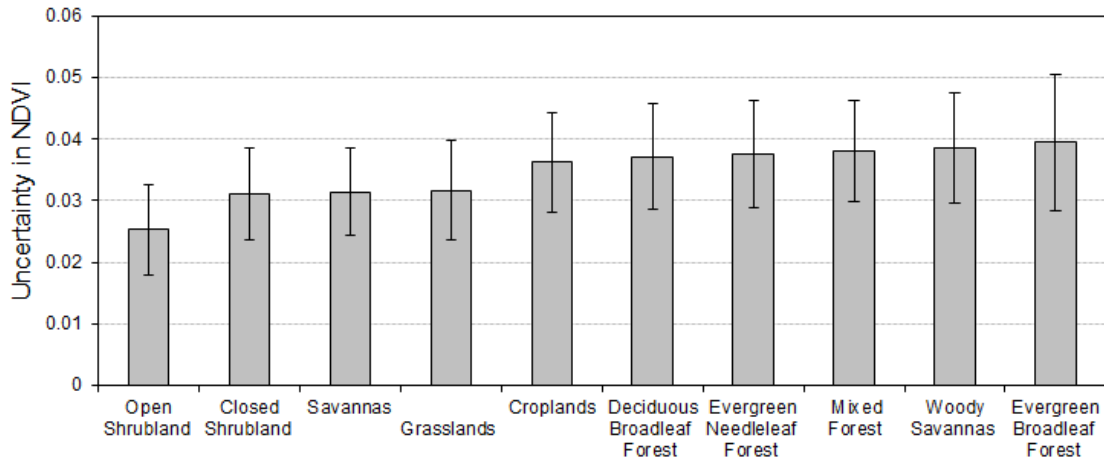
Fig. 5-5: *Mean uncertainty of each land cover type. Deserts, urban areas, wetlands, and the pixels with less than 30 data points were excluded from the analysis.*

The summary, the AVHRR NDVI uncertainty estimates for each land cover type (Fig. 5-5; 5-4) revealed that the uncertainty varies from 0.025 NDVI units for open shrubland to 0.04 NDVI units for evergreen broadleaf forest. A closer examination of the uncertainty map (Fig. 5-3) revealed a considerable variability of uncertainty within each land cover type; this variability was observed to be primarily caused by a combination of atmospheric conditions, surface vegetation conditions, and topography.

One of the chief limitations for location specific uncertainty estimation, that is estimation of uncertainty at an individual AVHRR pixel, is the unavailability of adequate data for valid application of the statistical framework defined in section 1.2.8. Due to this it was not possible to estimate uncertainty in many regions like large tracts of tropical forests, tundra, and boreal forests (Fig. 5-3).

At many sites considerable seasonal variability in uncertainty was also observed. This seasonal variability showed a strong correlation with the magnitude of NDVI. One can account for this seasonal variability by estimating uncertainty for individual months, seasons, or NDVI bins (e.g. 0 to 0.2, 0.4 to 0.5, and 0.8 to 1.0 NDVI units, etc.) separately. However such an endeavor is again hindered by inadequate data availability. One technique to overcome this problem is to estimate uncertainty for whole regions or sub-regions instead of individual pixels.

5.3. Impact of Uncertainty in AVHRR-NDVI Data on Inter-annual Trends

The inter-annual trends in AVHRR NDVI data are generally estimated using linear (ordinary least squares) regression (Donohue et al., 2009; Jia et al., 2003; Slayback et al., 2003; Piao et al. 2006; Young and Harris 2005). The uncertainty in the inter-annual trend estimated using this technique depends not only on the magnitude of uncertainty in AVHRR NDVI data (measurement error) but also on the coefficient of determination (R-squared). Coefficient of determination is greatly affected by the length of the time series. This understanding was used to quantify the impact of uncertainty in AVHRR NDVI data on inter-annual NDVI trends for various lengths of time-series using a Monte Carlo approach. During this analysis the data were assumed stationary and without temporal gaps. A sample of the results, form the Monte Carlo simulations, is presented in Table 5-1. These results can be utilized to translate the magnitude of NDVI uncertainty to an estimate of the minimum change in NDVI that can be considered significant over a given time period.

NDVI precision	Time Series Length	Minimum Valid NDVI Change (95% Confidence Interval)
0.02	20 Years	0.0310
0.03	20 Years	0.0466
0.04	20 Years	0.0621
0.06	20 Years	0.0931
0.02	10 Years	0.0439
0.03	10 Years	0.0659
0.04	10 Years	0.0879
0.06	10 Years	0.1318

Table 5-1: *Minimum Valid NDVI change for various degrees of NDVI uncertainty for 10 and 20 year time period*

For example it can be ascertained that, at 95% confidence interval, the uncertainty of 0.021 NDVI units for LTDR NDVI data in clear atmospheric conditions as reported in chapter 2 (Fig. 5-1) translates to an uncertainty of 0.046 and 0.032 NDVI units for the total observed change over a period of 10 and 20 years respectively. This implies that when using LTDR NDVI data even under clear atmospheric conditions the observed changes in NDVI must be at least 0.046 over 10 years and 0.032 over 20 years for the change to be significant. For average atmospheric conditions the observed changes in NDVI must be at least 0.081 over 10 years or 0.057 over 20 years.

5.4. Implications of the results

The results from the investigation of uncertainty in AVHRR NDVI are of considerable significance and suggest that the conclusions of several influential studies of inter-annual vegetation dynamics that have treated small differences in

AVHRR NDVI as indicators of significant change should be revisited. For example, Tucker et al., (2001) reported an increase of 0.031 and 0.033 NDVI units for a 10 year period (1982-1991) in the 45°-75° latitudinal zone of North America and Eurasia respectively. An increase of 0.036 and 0.026 NDVI units was also reported for the same regions during the 8 year time period between 1992 and 1999. Another study by Zhou et al., (2001) reported an increase of 0.046 and 0.032 NDVI units over North America and Eurasia respectively over a period of 19 years (1981-1999). Both of these studies used GIMMS dataset, which has uncertainty similar to TOA data. When examined in the context of the uncertainty in AVHRR NDVI reported in chapter 2 (Fig. 5-1), these NDVI changes cannot be considered significant. There are many similar examples where small changes in NDVI are reported as significant (Myneni et al. 1997; Slayback et al. 2003; Tucker et al. 1991).

The spatially explicit uncertainty estimates presented in Fig 5-3 provide a tool for location specific examination of the significance of the reported NDVI changes. For example, Donohue et al., (2009) reported an increase of 0.0182 fPAR units in 26 years (1981-2006) in Australia. This was estimated by averaging individual inter-annual fPAR trends for all the pixels in Australia. The fPAR data used in this study was derived from PAL and Commonwealth Scientific and Industrial Research Organization (CSIRO) AVHRR NDVI datasets (King et al. 2003: Donohue et al. 2008). The NDVI data were converted to fPAR using simple linear transformation equations. Here the relationship between the fPAR and LTDR AVHRR NDVI data was calculated in order to transform fPAR back to NDVI. The result was a change of 0.012 NDVI units over the 26 years. The average uncertainty in LTDR AVHRR

NDVI data for Australian continent was found to be 0.022 NDVI units. Using the technique presented in section 5.3, it was determined that a minimum change of 0.029 NDVI units over a period of 26 years is required for the change to be considered significant. The LTDR dataset has a much advanced processing when compared to the dataset used in the Donohue et al. (2009) study, so the uncertainty of 0.022 NDVI units is likely to be a substantial underestimation. Even if this underestimated uncertainty is considered valid for this dataset the NDVI increase of 0.012 observed by Donohue et al. (2009) is not significant.
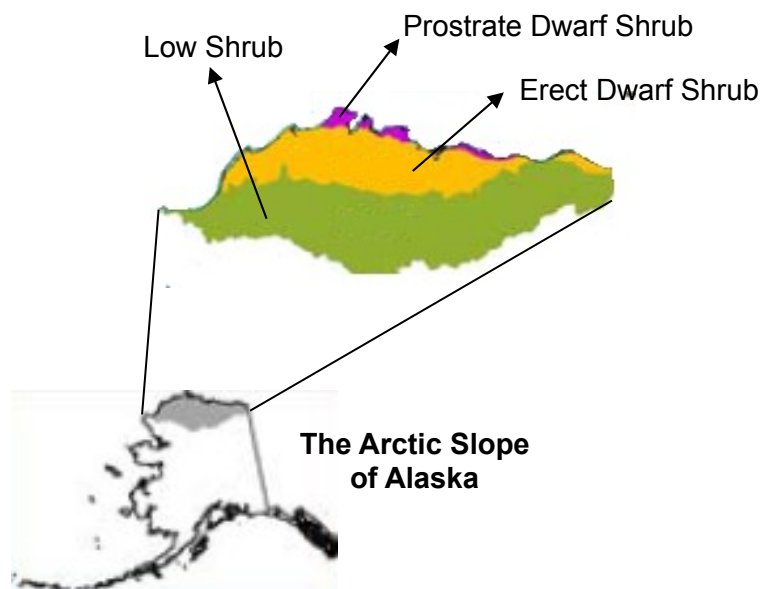
Fig. 5-6: *Bioclimatic subzones in the Arctic slope of Alaska investigated by Jia et al., (2003).*

As discussed earlier, in cases where inadequate availability of data makes estimation of location specific uncertainty impossible, the uncertainty can be estimated for a region or a sub-region as a whole. An example of the use of this

method is demonstrated here by estimating uncertainty in peak growing season NDVI data for the Erect Dwarf Shrub bioclimatic subzone of Alaskan Arctic slope (Fig. 5-6) (Jia et al. 2003). For this exercise uncertainty estimates for LTDR data were assumed applicable to GIMMS data used by Jia et al., (2003). The uncertainty in peak growing season NDVI data for the region was found to be 0.035 NDVI units. For the same bioclimatic subzone, Jia et al., (2003) reported an increase of 0.082 NDVI units over a period of 20 years (1981-2001). The uncertainty of 0.035 NDVI units implies that a minimum increase of 0.054 NDVI units is required for the change to be valid at 95 % confidence interval (Section 5.3). Because the reported increase of 0.082 NDVI units in yearly peak NDVI is more than this threshold (0.054) it can be considered significant.

The above two examples demonstrate the effectiveness of this method to interpret the significance of the inter-annual vegetation dynamics inferred from AVHRR NDVI data. This considerably enhances the value of the AVHRR NDVI data.

5.5. Future Directions

The uncertainty map presented in Fig. 5-3 does not cover large tracts of Earth surface and also does not account for temporal variability in uncertainty. This was primarily due to inadequate availability of cloud and snow free data. The discussion in sections 5.2 and 5.4 suggested that this problem can be overcome by estimating uncertainty for bioclimatic sub-zones instead of individual pixel locations. The bioclimatic sub-zones can be characterized by intersecting aerosol climatology maps with land-cover map, eco-region map, or even percent vegetation cover map. This approach will also provide adequate data for estimation of uncertainty for individual

NDVI bins or compositing periods to account for seasonal variability in uncertainty. A global uncertainty map produced using this approach can be of considerable relevance to the Earth system science research community.

The uncertainty in AVHRR NDVI data estimated by direct comparison with MODIS Aqua data does not account for the uncertainty MODIS data themselves, which can be as high as 0.017 NDVI (Vermote et al. 2006). A better spatial characterization of uncertainty in MODIS data and the quantification of impact of spatial and temporal aggregation can considerably improve the uncertainty estimates for AVHRR data.

Even after BRDF correction and vicarious calibration, evidence of substantial non-stationarity was found in AVHRR NDVI data at vegetated areas experiencing constant hazy atmosphere and in vegetated hilly regions (Fig. 5-2). Presence of non-stationarity leads to overestimation of uncertainty and also hampers the detection of inter-annual trends. Availability of a global map of degree of non-stationarity in AVHRR data could be of substantial value.

Most of the future use of AVHRR NDVI data is expected to be in conjunction with data from MODIS, or similar sensors like VIIRS (Gallo et al. 2005; Nagol et al. 2009; Pedelty et al. 2007; van Leeuwen et al. 1999). In this context not only the random component of uncertainty but the systematic bias also becomes relevant. A detailed study of this aspect of uncertainty can considerably improve the inter-calibration between NDVI data from AVHRR and MODIS instruments, as is being undertaken by the LTDR project.

Both empirical (Tucker et al. 2005) as well as analytical (van Leeuwen et al. 2006) equations have been developed for inter-calibration of AVHRR and MODIS data. Most of these do not account for spatial variability of the systematic bias caused by changes in surface and atmospheric conditions. By comparing AVHRR data directly to MODIS, more precise and location specific, inter-calibration equations can be developed. This kind of study would enhance the interoperability between AVHRR and MODIS datasets.

Bibliography

Abel, P., Guenther, B., Galimore, R.N., & Cooper, J.W. (1993). Calibration Results for NOAA-11 AVHRR Channel-1 And Channel-2 From Congruent Path Aircraft Observations. *Journal of Atmospheric and Oceanic Technology, 10*, 493-508

Alcaraz-Segura, D., Liras, E., Tabik, S., Paruelo, J., Cabello, J. (2010). Evaluating the Consistency of the 1982-1999 NDVI Trends in the Iberian Peninsula across Four Time-series Derived from the AVHRR Sensor: LTDR, GIMMS, FASIR, and PAL-II . *Sensors, 10, 1291-1314*

Anyamba, A., & Eastman, J.R. (1996). Interannual variability of NDVI over Africa and its relation to El Nino Southern Oscillation. *International Journal of Remote Sensing, 17*, 2533-2548

Bacour, C., Breon, F.M., & Maignan, F. (2006). Normalization of the directional effects in NOAA-AVHRR reflectance measurements for an improved monitoring of vegetation cycles. *Remote Sensing of Environment, 102*, 402-413

Baldocchi, D., Falge, E., Gu, L.H., Olson, R., Hollinger, D., Running, S., Anthoni, P., Bernhofer, C., Davis, K., Evans, R., Fuentes, J., Goldstein, A., Katul, G., Law, B., Lee, X.H., Malhi, Y., Meyers, T., Munger, W., Oechel, W., U, K.T.P., Pilegaard, K., Schmid, H.P., Valentini, R., Verma, S., Vesala, T., Wilson, K., & Wofsy, S. (2001). FLUXNET: A new tool to study the temporal and spatial variability of ecosystem-scale carbon dioxide, water vapor, and energy flux densities. *Bulletin of the American Meteorological Society, 82*, 2415-2434

Barbosa, P.M., Gregoire, J.M., & Pereira, J.M.C. (1999). An algorithm for extracting burned areas from time series of AVHRR GAC data applied at a continental scale. *Remote Sensing of Environment, 69*, 253-263

Bell, S. (1999). Measurement Good Practice Guide No. 11. A Beginner's Guide to Uncertainty of Measurement. Tech. rep., National Physical Laboratory

Bounoua, L., Collatz, G.J., Los, S.O., Sellers, P.J., Dazlich, D.A., Tucker, C.J., & Randall, D.A. (2000). Sensitivity of climate to changes in NDVI. *Journal of Climate, 13*, 2277-2292

Brown, M.E., Pinzon, J.E., Didan, K., Morisette, J.T., & Tucker, C.J. (2006). Evaluation of the consistency of long-term NDVI time series derived from AVHRR, SPOT-Vegetation, SeaWiFS, MODIS, and Landsat ETM+ sensors. *IEEE Transactions on Geoscience and Remote Sensing, 44*, 1787-1793

Cao, M.K., Prince, S.D., Small, J., & Goetz, S.J. (2004). Remotely sensed interannual variations and trends in terestrial net primary productivity 1981-2000. *Ecosystems, 7*, 233-242

Cihlar, J., Chen, J.M., Li, Z., Huang, F., Latifovic, R., & Dixon, R. (1998). Can interannual land surface signal be discerned in composite AVHRR data? *Journal of Geophysical Research-Atmospheres, 103*, 23163-23172

Cihlar, J., Manak, D., & Diorio, M. (1994). Evaluation of Compositing Algorithms for AVHRR Data over Land. *IEEE Transactions on Geoscience and Remote Sensing, 32*, 427-437

Cohen, W.B., & Justice, C.O. (1999). Validating MODIS terrestrial ecology products: Linking in situ and satellite measurements. *Remote Sensing of Environment, 70*, 1-3

Deering, D.W., Middleton, E.M., Irons, J.R., Blad, B.L., Waltershea, E.A., Hays, C.J., Walthall, C., Eck, T.F., Ahmad, S.P., & Banerjee, B.P. (1992). Prairie Grassland Bidirectional Reflectances Measured by Different Instruments at the Fife Site. *Journal of Geophysical Research-Atmospheres, 97*, 18887-18903

DeFries, R., Hansen, M., & Townshend, J. (1995). Global discrimination of land cover types from metrics derived from AVHRR pathfinder data. *Remote Sensing of Environment, 54*, 209-222

DeFries, R.S., Townshend, J.R.G., & Hansen, M.C. (1999). Continuous fields of vegetation characteristics at the global scale at 1-km resolution. *Journal of Geophysical Research-Atmospheres, 104*, 16911-16923

Donohue, R.J., McVicar, T.R., & Roderick, M.L. (2009). Climate-related trends in Australian vegetation cover as inferred from satellite observations, 1981-2006. *Global Change Biology, 15*, 1025-1039

Eidenshink, J. (2006). A 16-year time series of 1 km AVHRR satellite data of the conterminous United States and Alaska. *Photogrammetric Engineering and Remote Sensing, 72*, 1027-1035

Eidenshink, J.C. (1992). The 1990 Conterminous United-States AVHRR Data Set. *Photogrammetric Engineering and Remote Sensing, 58*, 809-813

Eidenshink, J.C., & Faundeen, J.L. (1994). The 1km AVHRR Global Land Data Set - 1st Stages in Implementation. *International Journal of Remote Sensing, 15*, 3443-3462

Eklundh, L.R. (1995). Noise Estimation in NOAA AVHRR Maximum-Value Composite NDVI Images. *International Journal of Remote Sensing, 16*, 2955-2962

El Saleous, N.Z., Vermote, E.F., Justice, C.O., Townshend, J.R.G., Tucker, C.J., & Goward, S.N. (2000). Improvements in the global biospheric record from the Advanced Very High Resolution Radiometer (AVHRR). *International Journal of Remote Sensing, 21*, 1251-1277

Fang, J.Y., Piao, S., Field, C.B., Pan, Y., Guo, Q.H., Zhou, L.M., Peng, C.H., & Tao, S. (2003). Increasing net primary production in China from 1982 to 1999. *Frontiers in Ecology and the Environment, 1*, 293-297

Fensholt, R., Nielsen, T.T., & Stisen, S. (2006a). Evaluation of AVHRR PAL and GIMMS 10-day composite NDVI time series products using SPOT-4 vegetation data for the African continent. *International Journal of Remote Sensing, 27*, 2719-2733

Fensholt, R., Rasmussen, K., Nielsen, T.T., & Mbow, C. (2009). Evaluation of earth observation based long term vegetation trends - Intercomparing NDVI time series trend analysis consistency of Sahel from AVHRR GIMMS, Terra MODIS and SPOT VGT data. *Remote Sensing of Environment, 113*, 1886-1898

Fensholt, R., & Sandholt, I. (2005). Evaluation of MODIS and NOAA AVHRR vegetation indices with in situ measurements in a semi-arid environment. *International Journal of Remote Sensing, 26*, 2561-2594

Fensholt, R., Sandholt, I., & Stisen, S. (2006b). Evaluating MODIS, MERIS, and VEGETATION - Vegetation indices using in situ measurements in a semiarid environment. *IEEE Transactions on Geoscience and Remote Sensing, 44*, 1774-1786

Franklin, J.F., Bledsoe, C.S., & Callahan, J.T. (1990). Contributions of the Long-Term Ecological Research-Program - an Expanded Network of Scientists, Sites, and Programs Can Provide Crucial Comparative Analyses. *Bioscience, 40*, 509-523

Gallo, K., Li, L., Reed, B., Eidenshink, J., & Dwyer, J. (2005). Multi-platform comparisons of MODIS and AVHRR normalized difference vegetation index data. *Remote Sensing of Environment, 99*, 221-231

Gorman, A.J., & McGregor, J. (1994). Some Considerations for Using AVHRR Data in Climatological Studies - Instrument Performance. *International Journal of Remote Sensing, 15*, 549-565

Goward, S.N., Dye, D.G., Turner, S., & Yang, J. (1993). Objective Assessment of the NOAA Global Vegetation Index Data Product. *International Journal of Remote Sensing, 14*, 3365-3394

Gutman, G., Tarpley, D., Ignatov, A., & Olson, S. (1995). The Enhanced NOAA Global Land Dataset from the Advanced Very High-Resolution Radiometer. *Bulletin of the American Meteorological Society, 76*, 1141-1156

Gutman, G.G. (1999). On the use of long-term global data of land reflectances and vegetation indices derived from the advanced very high resolution radiometer. *Journal of Geophysical Research-Atmospheres, 104*, 6241-6255

Hatfield, J.L., Kanemasu, E.T., Asrar, G., Jackson, R.D., Pinter, P.J., Reginato, R.J., & Idso, S.B. (1985). Leaf-Area Estimates from Spectral Measurements over Various Planting Dates of Wheat. *International Journal of Remote Sensing, 6*, 167-175

Heidinger, A.K., Cao, C.Y., & Sullivan, J.T. (2002). Using Moderate Resolution Imaging Spectrometer (MODIS) to calibrate advanced very high resolution radiometer reflectance channels. *Journal of Geophysical Research-Atmospheres, 107*

Hicke, J.A., Asner, G.P., Randerson, J.T., Tucker, C., Los, S., Birdsey, R., Jenkins, J.C., Field, C., & Holland, E. (2002). Satellite-derived increases in net primary productivity across North America, 1982-1998. *Geophysical Research Letters, 29*

Hodges, J. (2002). MOD12 Land Cover and Land Cover Dynamics Products User Guide. *Department of Geography, Boston University*

Holben, B.N. (1986). Characteristics of Maximum-Value Composite Images from Temporal AVHRR Data. *International Journal of Remote Sensing, 7*, 1417-1434

Holben, B.N., Kaufman, Y.J., & Kendall, J.D. (1990). NOAA-11 AVHRR Visible and Near-IR Inflight Calibration. *International Journal of Remote Sensing, 11*, 1511-1519

Holben, B.N., Tanre, D., Smirnov, A., Eck, T.F., Slutsker, I., Abuhassan, N., Newcomb, W.W., Schafer, J.S., Chatenet, B., Lavenu, F., Kaufman, Y.J., Castle, J.V., Setzer, A., Markham, B., Clark, D., Frouin, R., Halthore, R., Karneli, A., O'Neill, N.T., Pietras, C., Pinker, R.T., Voss, K., & Zibordi, G. (2001). An emerging ground-based aerosol climatology: Aerosol optical depth from AERONET. *Journal of Geophysical Research-Atmospheres, 106*, 12067-12097

Huete, A.R., & Jackson, R.D. (1987). Suitability of Spectral Indexes for Evaluating Vegetation Characteristics on Arid Rangelands. *Remote Sensing of Environment, 23*, 213-&

Ichii, K., Kawabata, A., & Yamaguchi, Y. (2002). Global correlation analysis for NDVI and climatic variables and NDVI trends: 1982-1990. *International Journal of Remote Sensing, 23*, 3873-3878

James, M.E., & Kalluri, S.N.V. (1994). The Pathfinder AVHRR Land Data Set - an Improved Coarse Resolution Data Set for Terrestrial Monitoring. *International Journal of Remote Sensing, 15*, 3347-3363

Ji, L., Gallo, K., Eidenshink, J.C., & Dwyer, J. (2008). Agreement evaluation of AVHRR and MODIS 16-day composite NDVI data sets. *International Journal of Remote Sensing, 29*, 4839-4861

Jia, G.S.J., Epstein, H.E., & Walker, D.A. (2003). Greening of arctic Alaska, 1981-2001. *Geophysical Research Letters, 30*

Jin, M. (2004). Analysis of land skin temperature using AVHRR observations. *Bulletin of the American Meteorological Society, 85*, 587-+

Jupp, D.L.B., & Strahler, A.H. (1991). A Hotspot Model for Leaf Canopies. *Remote Sensing of Environment, 38*, 193-210

Justice, C., Belward, A., Morisette, J., Lewis, P., Privette, J., & Baret, F. (2000). Developments in the 'validation' of satellite sensor products for the study of the land surface. *International Journal of Remote Sensing, 21*, 3383-3390

Kangas, M., Heikinheimo, M., & Laine, V. (2001). Accuracy of NOAA AVHRR-based surface reflectance over a winter-time boreal surface - comparison with aircraft measurements and land-cover information. *Theoretical and Applied Climatology, 70*, 231-244

Kaufman, Y.J., & Holben, B.N. (1993). Calibration of the AVHRR Visible And Near-IR Bands By Atmospheric Scattering, Ocean Glint And Desert Reflection. *International Journal of Remote Sensing, 14*, 21-52

Kaufmann, R.K., Zhou, L.M., Knyazikhin, Y., Shabanov, N.V., Myneni, R.B., & Tucker, C.J. (2000). Effect of orbital drift and sensor changes on the time series of AVHRR vegetation index data. *IEEE Transactions on Geoscience and Remote Sensing, 38*, 2584-2597

Kidwell, K.B. (1994). Global Vegetation Index User Guide, U.S. Dept. of Commerce, NOAA/NESDIS, Satellite Data Services Division, Nat. Climatic Data Center, Asheville, N. C.

Kidwell, K.B. (1997). NOAA Global Vegetation Index User's Guide (Revision), U.S. Dept. of Commerce, NOAA/NESDIS, Climate Services Division, Nat. Climatic Data Center, Suitland, Md.

Kidwell, K.B. (1998). NOAA polar orbiter data user's guide. U.S. Department of Commerce, NESDIS. *NOAA, National Climatic Data Center, Satellite Data Services Division, Washington, D.C.*

Kogan, F.N., & Zhu, X. (2001). Evolution of long-term errors in NDVI time series: 1985-1999. *Calibration and Characterization of Satellite Sensors and Accuracy of Derived Physical Parameters, 28*, 149-153

Lambin, E.F., & Ehrlich, D. (1997). Land-cover changes in sub-Saharan Africa (1982-1991): Application of a change index based on remotely sensed surface temperature and vegetation indices at a continental scale. *Remote Sensing of Environment, 61*, 181-200

Latifovic, R., Cihlar, J., & Chen, J. (2003). A comparison of BRDF models for the normalization of satellite optical data to a standard sun-target-sensor geometry. *IEEE Transactions on Geoscience and Remote Sensing, 41*, 1889-1898

Latifovic, R., Trishchenko, A.P., Chen, J., Park, W.B., Khlopenkov, K.V., Fernandes, R., Pouliot, D., Ungureanu, C., Luo, Y., Wang, S., Davidson, A., & Cihlar, J. (2005). Generating historical AVHRR 1 km baseline satellite data records over Canada suitable for climate change studies. *Canadian Journal of Remote Sensing, 31*, 324-346

Lee, R., Yu, F., Price, K.P., Ellis, J., & Shi, P. (2002). Evaluating vegetation phenological patterns in Inner Mongolia using NDVI time-series analysis. *International Journal of Remote Sensing, 23*, 2505-2512

Liu, W.T.H., Massambani, O., & Nobre, C.A. (1994). Satellite Recorded Vegetation Response to Drought in Brazil. *International Journal of Climatology, 14*, 343-354

Loeb, N.G. (1997). In-flight calibration of NOAA AVHRR visible and near-IR bands over Greenland and Antarctica. *International Journal of Remote Sensing, 18*, 477-490

Los, S.O. (1998). Estimation of the ratio of sensor degradation between NOAA AVHRR channels 1 and 2 from monthly NDVI composites. *IEEE Transactions on Geoscience and Remote Sensing, 36*, 206-213

Los, S.O., North, P.R.J., Grey, W.M.F., & Barnsley, M.J. (2005). A method to convert AVHRR Normalized Difference Vegetation Index time series to a standard viewing and illumination geometry. *Remote Sensing of Environment, 99*, 400-411

Lucht, W., Prentice, I.C., Myneni, R.B., Sitch, S., Friedlingstein, P., Cramer, W., Bousquet, P., Buermann, W., & Smith, B. (2002). Climatic control of the high-latitude vegetation greening trend and Pinatubo effect. *Science, 296*, 1687-1689

Malingreau, J.P., & Belward, A.S. (1994). Recent Activities in the European-Community for the Creation and Analysis of Global AVHRR Data Sets. *International Journal of Remote Sensing, 15*, 3397-3416

McPeters, R.D., & Labow, G.J. (1996). An assessment of the accuracy of 14.5 years of Nimbus 7 TOMS Version 7 ozone data by comparison with the Dobson network. *Geophysical Research Letters, 23*, 3695-3698

Morisette, J.T., Privette, J.L., & Justice, C.O. (2002). A framework for the validation of MODIS Land products. *Remote Sensing of Environment, 83*, 77-96

Myneni, R.B., Keeling, C.D., Tucker, C.J., Asrar, G., & Nemani, R.R. (1997a). Increased plant growth in the northern high latitudes from 1981 to 1991. *Nature, 386*, 698-702

Myneni, R.B., Nemani, R.R., & Running, S.W. (1997b). Estimation of global leaf area index and absorbed par using radiative transfer models. *IEEE Transactions on Geoscience and Remote Sensing, 35*, 1380-1393

Myneni, R.B., Tucker, C.J., Asrar, G., & Keeling, C.D. (1998). Interannual variations in satellite-sensed vegetation index data from 1981 to 1991. *Journal of Geophysical Research-Atmospheres, 103*, 6145-6160

Nagol, J.R., Vermote, E.F., & Prince, S.D. (2009). Effects of atmospheric variation on AVHRR NDVI data. *Remote Sensing of Environment, 113*, 392-397

North, P., Plummer, S.E., Deering, D.W., & Leroy, M. (1996). Validation of a BRDF model in Boreal forest. *Proc. of International Geoscience and Remote Sensing Symposium. Lincoln, Nebraska, USA (27– 31 May, 1996).*

North, P.R.J. (1996). Three-dimensional forest light interaction model using a Monte Carlo method. *IEEE Transactions on Geoscience and Remote Sensing, 34*, 946-956

Ouaidrari, H., El Saleous, N., Vermote, E.F., Townshend, J.R., & Goward, S.N. (2003). AVHRR Land Pathfinder II (ALP II) data set: evaluation and inter-comparison with other data sets. *International Journal of Remote Sensing, 24*, 135-142

Paruelo, J.M., Garbulsky, M.F., Guerschman, J.P., & Jobbagy, E.G. (2004). Two decades of Normalized Difference Vegetation Index changes in South America: identifying the imprint of global change. *International Journal of Remote Sensing, 25*, 2793-2806

Pedelty, J., Masuoka, E.B., Brown, M.E., Pinzon, J., Tucker, C.J., Vermote, E.F., Prince, S.D., Justice, C.O., Nagol, J., Roy, D., Junchang, J., Schaaf, C., Jicheng, L., Privette, J.L., & Pinheiro, A. (2007). Generating a long-term land data record from the AVHRR and MODIS Instruments. *Geoscience and Remote Sensing Symposium, 2007. IGARSS 2007. IEEE International*, 1021-1025

Piao, S.L., Fang, J.Y., Ji, W., Guo, Q.H., Ke, J.H., & Tao, S. (2004). Variation in a satellite-based vegetation index in relation to climate in China. *Journal of Vegetation Science, 15*, 219-226

Piao, S.L., Fang, J.Y., Zhou, L.M., Guo, Q.H., Henderson, M., Ji, W., Li, Y., & Tao, S. (2003). Interannual variations of monthly and seasonal normalized difference vegetation index (NDVI) in China from 1982 to 1999. *Journal of Geophysical Research-Atmospheres, 108*

Piao, S.L., Mohammat, A., Fang, J.Y., Cai, Q., & Feng, J.M. (2006). NDVI-based increase in growth of temperate grasslands and its responses to climate changes in China. *Global Environmental Change-Human and Policy Dimensions, 16*, 340-348

Pinty, B., Widlowski, J.L., Taberner, M., Gobron, N., Verstraete, M.M., Disney, M., Gascon, F., Gastellu, J.P., Jiang, L., Kuusk, A., Lewis, P., Li, X., Ni-Meister,

W., Nilson, T., North, P., Qin, W., Su, L., Tang, S., Thompson, R., Verhoef, W., Wang, H., Wang, J., Yan, G., & Zang, H. (2004). Radiation Transfer Model Intercomparison (RAMI) exercise: Results from the second phase. *Journal of Geophysical Research-Atmospheres, 109*

Pinzon, J., Brown, M.E., & Tucker, C.J. (2005). Satellite time series correction of orbital drift artifacts using empirical mode decomposition. *In EMD and its Applieations, N.E.Huang and SS.P, Shen (Eds) (Singapore: World Scientific Publishers)*

Pouliot, D., Latifovic, R., Fernandes, R., & Olthof, I. (2010). Evaluation of compositing period and AVHRR and MERIS combination for improvement of spring phenology detection in deciduous forests. *Remote Sensing of Environment*

Prihodko, L., & Goward, S.N. (1997). Estimation of air temperature from remotely sensed surface observations. *Remote Sensing of Environment, 60*, 335-346

Prince, S.D., & Goward, S.N. (1995). Global primary production: A remote sensing approach. *Journal of Biogeography, 22*, 815-835

Privette, J.L., Eck, T.F., & Deering, D.W. (1997). Estimating spectral albedo and nadir reflectance through inversion of simple BRDF models with AVHRR/MODIS-like data. *Journal of Geophysical Research-Atmospheres, 102*, 29529-29542

Privette, J.L., Fowler, C., Wick, G.A., Baldwin, D., & Emery, W.J. (1995). Effects of Orbital Drift on Advanced Very High-Resolution Radiometer Products -

Normalized Difference Vegetation Index and Sea-Surface Temperature. *Remote Sensing of Environment, 53*, 164-171

Rao, C.R.N., & Chen, J. (1995). INTERSATELLITE CALIBRATION LINKAGES FOR THE VISIBLE AND NEAR-INFARED CHANNELS OF THE ADVANCED VERY HIGH-RESOLUTION RADIOMETER ON THE NOAA-7, NOAA-9, AND NOAA-11 SPACECRAFT. *International Journal of Remote Sensing, 16*, 1931-1942

Rao, C.R.N., & Chen, J.H. (1996). Post-launch calibration of the visible and near-infrared channels of the advanced very high resolution radiometer on the NOAA-14 spacecraft. *International Journal of Remote Sensing, 17*, 2743-2747

Robel, J. (2007). NOAA KLM USER'S GUIDE (with NOAA-N,-P SUPPLEMENT). U.S. Department of Commerce, NESDIS. *NOAA, National Climatic Data Center, Satellite Data Services Division, Washington, D.C.*

Roujean, J.L., Leroy, M., & Deschamps, P.Y. (1992). A Bidirectional Reflectance Model of the Earths Surface for the Correction of Remote-Sensing Data. *Journal of Geophysical Research-Atmospheres, 97*, 20455-20468

Rouse, J.W., Haas, R.H., Jr, Schell, J.A., & Deering, D.W. (1973). Monitoring vegetation systems in the Great Plains with ERTS. *Third ERTS Symposium, NASA, SP-351* 309-317

Runnstrom, M.C. (2000). Is northern China winning the battle against desertification? Satellite remote sensing as a tool to study biomass trends on the Ordos Plateau in semiarid China. *Ambio, 29*, 468-476

Sellers, P.J., Los, S.O., Tucker, C.J., Justice, C.O., Dazlich, D.A., Collatz, G.J., & Randall, D.A. (1996). A revised land surface parameterization (SiB2) for atmospheric GCMs .2. The generation of global fields of terrestrial biophysical parameters from satellite data. *Journal of Climate, 9*, 706-737

Slayback, D.A., Pinzon, J.E., Los, S.O., & Tucker, C.J. (2003). Northern hemisphere photosynthetic trends 1982-99. *Global Change Biology, 9*, 1-15

Stellmes, M., Udelhoven, T., Roder, A., Sonnenschein, R., & Hill, J. (2010). Dryland observation at local and regional scale - Comparison of Landsat TM/ETM plus and NOAA AVHRR time series. *Remote Sensing of Environment, 114*, 2111-2125

Stockli, R., & Vidale, P.L. (2004). European plant phenology and climate as seen in a 20-year AVHRR land-surface parameter dataset. *International Journal of Remote Sensing, 25*, 3303-3330

Stowe, L.L., Davis, P., & McClain, E.P. (1995). Evaluating the Clavr (Clouds from AVHRR) Phase-I Cloud Cover Experimental Product. *Satellite Monitoring of the Earth's Surface and Atmosphere, 16*, 21-24

Swap, B., Suttles, T., Annegarn, H., Scorgie, Y., Closs, J., Privette, J., & B., C. (2000). Report on SAFARI 2000 outreach activities, intensive field campaign planning meeting, and data management workshop. *Earth Observer, 12* 21–25

Swinnen, E., Eerens, H., Heyns, W., Piccard, I., Viaene, P., & Claes, P. (2007). An integrated long time series of 1 km resolution NDVI for Europe from the NOAA-AVHRR and SPOT-VEGETATION sensors. *Proceedings of MultiTemp 2007: 4th International workshop on the analysis of multi-*

temporal remote sensing images", 18-20 July, 2007, Leuven, Belgium. Eds. De Lannoy G. et al., Leuven, Gent: Katholieke Universiteit Leuven, Universiteit Gent, ISBN 1-4244-0846-6 (2007).

Tanre, D., Holben, B.N., & Kaufman, Y.J. (1992). ATMOSPHERIC CORRECTION ALGORITHM FOR NOAA-AVHRR PRODUCTS - THEORY AND APPLICATION. *IEEE Transactions on Geoscience and Remote Sensing, 30*, 231-248

Teillet, P.M., El Saleous, N., Hansen, M.C., Eidenshink, J.C., Justice, C.O., & Townshend, J.R.G. (2000). An evaluation of the global 1-km AVHRR land dataset. *International Journal of Remote Sensing, 21*, 1987-2021

Teillet, P.M., & Holben, B.N. (1994). Towards Operational Radiometric Calibration of NOAA AVHRR Imagery in the Visible and Near-Infrared Channels. *Canadian Journal of Remote Sensing, 20*, 1-10

Teillet, P.M., Slater, P.N., Ding, Y., Santer, R.P., Jackson, R.D., & Moran, M.S. (1990). 3 METHODS FOR THE ABSOLUTE CALIBRATION OF THE NOAA AVHRR SENSORS IN-FLIGHT. *Remote Sensing of Environment, 31*, 105-120

Townshend, J.R.G., & Tucker, C.J. (1981). Utility of AVHRR of NOAA 6 and 7 for vegetation mapping. *In, Matching Remote Sensing Technologies and their Applications (Proceedings of an international Conference London, December 1981) (p. 97)*

Tucker, C.J. (1979). Red and Photographic Infrared Linear Combinations for Monitoring Vegetation. *Remote Sensing of Environment, 8*, 127-150

Tucker, C.J., Dregne, H.E., & Newcomb, W.W. (1991). Expansion and Contraction of the Sahara Desert from 1980 to 1990. *Science, 253*, 299-301

Tucker, C.J., Gatlin, J.A., & Schneider, S.R. (1984). Monitoring Vegetation in the Nile Delta with NOAA-6 and NOAA-7 AVHRR Imagery. *Photogrammetric Engineering and Remote Sensing, 50*, 53-61

Tucker, C.J., Pinzon, J.E., Brown, M.E., Slayback, D.A., Pak, E.W., Mahoney, R., Vermote, E.F., & El Saleous, N. (2005). An extended AVHRR 8-km NDVI dataset compatible with MODIS and SPOT vegetation NDVI data. *International Journal of Remote Sensing, 26*, 4485-4498

Tucker, C.J., Slayback, D.A., Pinzon, J.E., Los, S.O., Myneni, R.B., & Taylor, M.G. (2001). Higher northern latitude normalized difference vegetation index and growing season trends from 1982 to 1999. *International Journal of Biometeorology, 45*, 184-190

van Leeuwen, W.J.D., Huete, A.R., & Laing, T.W. (1999). MODIS vegetation index compositing approach: A prototype with AVHRR data. *Remote Sensing of Environment, 69*, 264-280

Vermote, E., Justice, C.O., & Breon, F.M. (2009a). Towards a Generalized Approach for Correction of the BRDF Effect in MODIS Directional Reflectances. *IEEE Transactions on Geoscience and Remote Sensing, 47*, 898-908

Vermote, E., & Kaufman, Y.J. (1995). Absolute Calibration Of AVHRR Visible And Near-Infrared Channels Using Ocean And Cloud Views. *International Journal of Remote Sensing, 16*, 2317-2340

Vermote, E., Kotchenova, S., & Roa, J. (2006). MODIS surface radiation data products maintenance and refinement. *MODIS Science Team Meeting, College Park, Maryland, Octuber 31st - Novemeber 2nd , Department of Geography, University of Maryland, NASA/GSFC Code 614.5.*

Vermote, E.F., Justice, C.O., Csiszar, I., Eidenshink, J.C., Myneni, R.B., Baret, F., Masuoka, E., Wolfe, R., & Devadiga, S. (2009b). A Terrestrial Surface Climate Data Record for Global Chage Studies, American Geophysical Union, Annual Fall Meeting, December 2009, San Francisco, California

Vermote, E.F., & Kotchenova, S. (2008). Atmospheric correction for the monitoring of land surfaces. *Journal of Geophysical Research-Atmospheres, 113*

Vermote, E.F., & Saleous, N.Z. (1997). Data Pre-Processing: Stratospheric Aerosol Perturbing Effect on the Remote Sensing of Vegetation: Correction Method for the Composite NDVI after the Pinatubo Eruption. *Remote Sensing Reviews, 15*, 7-21.

Vermote, E.F., & Saleous, N.Z. (2006a). Calibration of NOAA16 AVHRR over a desert site using MODIS data. *Remote Sensing of Environment, 105*, 214-220

Vermote, E.F., & Saleous, N.Z. (2006b). Operational Atmospheric Correction of MODIS Visible to Middle Infrared Land Surface Data in the Case of an Infinite Lambertian Target. *Book Chapter in "Earth Science Satellite Remote Sensing", J. J.Qu, W. Gao. M. Kafatos, R.E. Murphy, V. V. Salomonson,(Eds), 2006., publisher Springer.*

Vermote, E.F., Tanre, D., Deuze, J.L., Herman, M., & Morcrette, J.J. (1997). Second Simulation of the Satellite Signal in the Solar Spectrum, 6S: An overview. *IEEE Transactions on Geoscience and Remote Sensing, 35*, 675-686

Vicente-Serrano, S.M., & Heredia-Laclaustra, A. (2004). NAO influence on NDVI trends in the Iberian peninsula (1982-2000). *International Journal of Remote Sensing, 25*, 2871-2879

Young, S.S., & Harris, R. (2005). Changing patterns of global-scale vegetation photosynthesis, 1982-1999. *International Journal of Remote Sensing, 26*, 4537-4563

Yu, F.F., Price, K.P., Ellis, J., & Shi, P.J. (2003). Response of seasonal vegetation development to climatic variations in eastern central Asia. *Remote Sensing of Environment, 87*, 42-54

Zhou, L., Kaufmann, R.K., Tian, Y., Myneni, R.B., & Tucker, C.J. (2003). Relation between interannual variations in satellite measures of northern forest greenness and climate between 1982 and 1999. *Journal of Geophysical Research-Atmospheres, 108*

Zhou, L.M., Tucker, C.J., Kaufmann, R.K., Slayback, D., Shabanov, N.V., & Myneni, R.B. (2001). Variations in northern vegetation activity inferred from satellite data of vegetation index during 1981 to 1999. *Journal of Geophysical Research-Atmospheres, 106*, 20069-20083.